Scaling effects of riparian peatlands on stable isotopes in runoff and DOC mobilization

C. Tunaley [1], D. Tetzlaff [1], and C. Soulsby [1]

[1] Northern Rivers Institute, School of Geosciences, University of Aberdeen, UK

Corresponding author: Claire Tunaley (claire.tunaley@abdn.ac.uk)

Abstract

We combined 13 months of daily isotope measurements in stream water with daily DOC and 15 minute FDOM (fluorescent component of dissolved organic matter) data at three nested scales to identify how riparian peatlands generate runoff and influence DOC dynamics in streams. We investigated how runoff generation processes in a small, riparian peatland-dominated headwater catchment (0.65 km^2) propagate to larger scales (3.2 km^2 and 31 km^2) with decreasing percentage of riparian peatland coverage. Isotope damping was most pronounced in the 0.65 km^2 headwater catchment due to high water storage in the organic soils encouraging tracer mixing. At the largest scale, stream flow and water isotope dynamics showed a more flashy response. The isotopic difference between the sites was most pronounced in the summer months when stream water signatures were enriched. During the winter months, the inter-site difference reduced. The isotopes also revealed evaporative fractionation in the peatland dominated catchment, in particular during summer low flows, which implied high hydrological connectivity in the form of constant seepage from the peatlands sustaining high baseflows at the headwater scale. This connectivity resulted in high DOC concentrations at the peatland site during baseflow (~ 5 mg l^{-1}). In contrast, at the larger scales, DOC was minimal during low flows (~2 mg l^{-1}) due to increased groundwater influence and the disconnection

between DOC sources and the stream. High frequency data also revealed diel variability during low flows. Insights into event dynamics through the analysis of hysteresis loops showed slight dilution on the rising limb, the strong influence of dry antecedent conditions and a quick recovery between events at the riparian peatland site. Again, these dynamics are driven by the tight coupling and high connectivity of the landscape to the stream. At larger scales, the disconnection between the landscape units increases and the variable connectivity controls runoff generation and DOC dynamics. The results presented here suggest that the processes occurring in riparian peatlands in headwater catchments are less evident at larger scales which may have implications for the larger scale impact of peatland restoration projects.

Keywords: Riparian peatland; Stable isotopes; Dissolved organic carbon; Scaling; High frequency; Connectivity.

1. Introduction

Knowledge of hydrological sources, flow paths and their connectivity is critical to understanding stream flow generation and the biogeochemical interactions that determine surface water quality. Peatlands store around one-third of the carbon in the terrestrial biosphere and are a major source of dissolved organic carbon (DOC) to streams (Gorham, 1991; Holden, 2005). It has been shown that a higher percentage of peat soils in a catchment correlate with higher DOC concentrations (Aitkenhead et al., 1999; Hope et al., 1997; Dawson et al., 2001). Of particular importance are the peat soils fringing the stream channel, in the riparian area (Billett and Cresser, 1992; Singh et al., 2015). Although riparian zones cover a relatively small area, previous research in headwater catchments has identified the disproportional influence they can have on runoff generation and water quality (Smart et al., 2001; Burt, 2005; Allan et al., 2008; Jencso et al., 2010; Vidon et al., 2010; Grabs et al., 2012). Riparian zones are critical areas of mixing where different catchment source waters integrate and generate the majority of annual discharge whilst also determining stream water chemistry (Morel et al., 2009; Birkel et al., 2011; Tetzlaff et al., 2014). Previous studies have identified the influence of the riparian zone on DOC dynamics. For example, Laudon et al. (2011) found that, in forested catchments, stream water DOC concentration was set by the last few meters of organic riparian soils along hillslope flow paths and a study by Dick et al. (2015) showed that riparian peatlands could account for up to 84 % of stream water DOC fluxes.

Given the importance of peatlands as a carbon store, it is vital to understand the hydrological functioning of these systems. Stable isotopes are proven tools for tracking the sources and flow paths of runoff (Buttle and Peters, 1997; Soulsby et al., 2000; Laudon et al., 2007; Capell et al., 2011). Their natural abundance and input-output transformation provide insights into the

mixing relationships between different water sources at a range of spatio-temporal scales (McGlynn and McDonnell, 2003; Soulsby et al., 2003; Rodgers et al., 2005). However, relatively few studies have used isotopes in peat-dominated catchments (Siegel and Glaser, 2006; Kværner and Kløve, 2008; Levy et al., 2014). Kværner and Kløve (2008) used isotopes to determine summer runoff generation in a boreal flat fen and identified different processes occurring during low flows and rainfall events, highlighting the importance of monitoring during different hydrological conditions. Recent studies in peatlands used isotopes to identify evaporation in surface waters (Carrer et al., 2015; Lessles et al., 2016; Sprenger et al., 2017). During evaporation, lighter isotopes are lost preferentially and residual water in peatland pools becomes relatively depleted in $\delta^{2}H$ compared to $\delta^{18}O$, plotting below the local meteoric water line (LMWL). Connectivity to these pools can lead to an evaporation signal translating to stream waters.

The mobilisation and transport of DOC from peat soils is dependent on the flow paths and connectivity between them and the stream channel network (Aitkenhead et al., 1999; McGlynn and McDonnell, 2003; Jencso et al., 2010; Inamdar et al., 2011; Laudon et al., 2011). The influence of peatlands is dependent on connectivity and position within the catchment and not just the areal extent (Laudon et al., 2011). The dominant sources and flow paths of water may switch under contrasting hydroclimatic conditions resulting in temporally varying DOC dynamics (Laudon et al., 2011; Singh et al., 2015). Isotopes, which help to understand runoff processes across a range of hydrologic conditions and scales, can be extremely helpful in understanding DOC dynamics (Tunaley et al., 2016). DOC concentrations can be highly variable over short periods of time and sampling at high frequencies to fully capture temporal dynamics was challenging prior to the development of optical sensors (Pellerin et al., 2011). Probes that measure the fluorescent component of dissolved organic matter (FDOM) provide

an *in-situ* proxy of DOC (Saraceno et al., 2009; Pellerin et al., 2011; Downing et al., 2012; Wilson et al., 2013). This allows seasonal, event and diel variations to be captured, and for DOC to be measured at timescales corresponding to hydrological and biogeochemical dynamics (Kirchner et al., 2004; Strohmeier et al., 2013; Tunaley et al., 2016).

In this context, it is clear that scaling remains one of the key challenges in catchment hydrology in determining how processes driving dynamics in headwater catchments translate to larger scales (Blöschl, 2001; Soulsby et al., 2006). Previous studies comparing catchments of different sizes have identified that catchment characteristics rather than catchment size *per se* are the major controls on runoff generation (Rodgers et al., 2005; Soulsby et al., 2006). Laudon et al. (2011), working in boreal Sweden, proposed that the proportion of forest versus wetland within a catchment determines downstream DOC dynamics irrespective of increases in catchment size. Generally, in most northern temperate environments, as catchment area increases towards the mesoscale (i.e. >10 km^2) the coverage of peat soils decreases (Soulsby et al., 2003; Dawson et al., 2011). However, uncertainties remain as to the scaling effects that peatland has on runoff generation and, in turn, DOC dynamics. This is important as peatland restoration projects in headwaters are often anticipated to moderate downstream flow regimes and improve water quality (Ramchunder et al., 2009; Haapalehto et al., 2014).

In this study, we combine daily stable isotope data with daily DOC and high-frequency FDOM at three nested scales in the 31 km^2 Girnock experimental catchment in the Cairngorm Mountains, Scotland. Our study builds upon previous work using isotope tracers (Tetzlaff et al, 2007; Birkel et al., 2011; Tetzlaff et al., 2014; Blumstock et al., 2015; Lessels et al., 2016) and DOC (Birkel et al., 2014; Dick et al., 2015; Tunaley et al., 2016). However, here we focus

on the first order (<1 km^2) headwaters of the Girnock that are dominated by a high percentage of riparian peatland. The overall aim was to determine how processes translate from such headwaters downstream to larger catchment scales. The study covers a 13 month period, capturing different seasons and hydrological conditions, to determine the spatio-temporal isotope dynamics in relation to runoff generation processes and associated DOC concentrations in streams. Furthermore, we progress on previous studies which mainly used weekly or daily data, by including high frequency DOC data. The study has two specific objectives: (1) to use isotopes to infer how riparian peatlands generate runoff and assess how that influence propagates to larger scales, and (2) evaluate how such changes in water sources and flow paths affect DOC dynamics in surface waters at different spatio-temporal scales. By addressing these research objectives we also comment on the potential and limitations of current peatland management strategies for regulating water quantity and quality and associated research needs.

2. Study site

The study was conducted in the Girnock Burn (31 km^2) experimental catchment situated in the Cairngorms National Park in Scotland. The catchment forms part of the wider drainage network of the Dee catchment. The Dee is the largest unregulated river in the UK and provides water supplies for 250,000 people with high water quality, an important salmon fishery and high conservation status. Mean annual precipitation is approximately 1000 mm which is evenly distributed throughout the year mainly falling in low intensity events (events < 10 mm d^{-1} account for > 50 % of annual inputs). Usually < 10 % of this precipitation falls as snow and there is no distinct snow melt period. Mean annual air temperature is around 8^{o}C and daily means range between 1 ^{o}C in winter to 12 ^{o}C in summer.

143 The study was conducted for three nested catchments: a 0.65 km^2 headwater catchment (HW1)
144 that drains into the Bruntland Burn (BB) (3.2 km^2), which is nested within the Girnock Burn
145 (GIR) (31 km^2) (Figure 1). In all three catchments, past glaciation has resulted in wide, flat
146 valley bottoms, filled with glacial till, surrounded by steep hillslopes (Figure 1a). Overlying
147 these deposits, the valley bottoms are dominated by histosols (peats and peaty gleys, Figure
148 1b), which remain close to saturation throughout the year (Tetzlaff et al., 2014). Therefore,
149 these soils are highly responsive to precipitation events by producing saturation excess
150 overland flow (Soulsby et al., 2015). The steeper hillslopes are dominated by more freely
151 draining podzols and rankers, which support groundwater recharge.

152

153 The catchments are described elsewhere (Tetzlaff et al., 2007; Birkel et al., 2014; Geris et al.,
154 2014; Blumstock et al., 2015). Here, we provide a brief description of the main differences
155 between the catchments, moving up in scale from HW1 to the GIR (Figure 1 & Table 1). The
156 smallest catchment HW1 is south facing and dominated by an extensive raised (ombrotrophic)
157 riparian peat bog (Blumstock et al., 2015; Dick et al., 2015). Small depressions in the bog
158 surface are filled with pools of water, which are dynamically connected/disconnected to the
159 stream channel via a peatland drainage network. The bog is surrounded by a groundwater-fed
160 fen area, receiving seepage from the adjacent steep hillslopes which mixes with peatland
161 waters. HW1 is the most peat-dominated of the catchments, with 15 % peat soils compared to
162 the BB and the GIR, which have 9 % and 4 %, respectively. More importantly, HW1 has the
163 highest percentage of peat soils fringing the stream channel (81 %) compared to the BB and
164 the GIR, with 53 % and 9 %, respectively. Geophysical surveys have indicated that the BB has
165 more extensive glacial drift deposits compared to the GIR with around 70 % of the catchment
166 covered with these deposits, which can be up to 40 meters deep in the valley bottoms (Soulsby
167 et al., 2016). In agreement with previous tracer studies by Hrachowitz et al. (2010) and Birkel

et al. (2014, 2011), these deposits result in larger catchment storage in the BB and higher groundwater influence compared to the GIR. This results in the GIR producing a more flashy response to precipitation events than the BB (Tetzlaff et al., 2007; Ali et al., 2014).

3. Data and Methods

3.1 Field measurements

Stream monitoring was conducted at the outlet of each of the catchments (Figure 1) from 14 May 2014 to 19 July 2015. Sampling at the GIR began slightly later on 12 June 2014. Daily stream samples were collected at 14:00 using ISCO 3700 autosamplers and analysed for stable isotopes. Integrated precipitation samples were collected every 24 hours from the BB site. Previous studies at the site have shown that the precipitation isotopic signature does not show spatial variability and has limited altitudinal effects (Tyler et al., 2007; Birkel et al., 2011). To prevent isotope fractionation within the samples, they were preserved using paraffin. Samples were analysed in the lab using a Los Gatos DLT-100 laser isotope analyser (precision of +/- 0.4 ‰ for δ^2H; +/-0.1 ‰ for $\delta^{18}O$) and results reported in the δ notation according to the Vienna Standard Mean Ocean Water. Due to the higher relative precision for δ^2H, we mostly used this in the analysis.

Separate stream samples were also collected at 14:00 for DOC analysis at the three catchments between 12 June 2014 and 1 July 2015 using equivalent autosamplers. Following filtration with 0.45 µm filters, samples were analyzed using a LABTOC Aqueous Carbon analyzer. The detection limit was 0.5 mg l^{-1}.To reduce the analytical load, around 10 random samples per site per month were analyzed.

Additionally, *in-situ* high frequency monitoring (15 minute) was also undertaken at the HW1 and BB outlets between 6 March 2015 and 3 August 2015. This was conducted using an EXO2 multi sonde (Xylem Inc, NY, USA) at the HW1 outlet and a TriOS optical sensor (TriOS Mess- und Datentechnik GmbH, Germany), logged to a Campbell Scientific CR800 datalogger, at the BB outlet. A TriOS optical sensor was also situated at the GIR outlet but due to persistent technical problems the data set was inadequate for comparison. Both probes measure FDOM; the fraction of DOC that absorbs light in the UV range of 365 nm (+/-5 nm) and emits at 480 nm (+/- 40 nm). The EXO2 sensor was re-calibrated every three months using quinine sulfate standards and expressed as quinine sulfate units (QSU). This probe also measured water temperature (ºC), electrical conductance (µS cm^{-1}), pH and turbidity (Formazin Nephelometric Unit (FNU)) which were calibrated on the same occasions as FDOM. The TriOS sensor was locally calibrated using quinine sulfate standards as per the instructions of the instrument manual. The EXO2 sonde had a wiper installed on the sensor to reduce the risk of biofouling and the TriOS probe was removed frequently for cleaning, however, biofouling was minimal.

Precipitation and stage height measurements were monitored at 15 minute intervals for the three sites using rain gauges and level recorders. Gaugings at the catchment outlets were frequently undertaken and subsequently, discharge was calculated at the three sites. Three Automatic Weather Stations in the BB had 0.2 mm tipping bucket gauges for rainfall estimates.

3.2 Data processing

The R programming language (R Core Team, 2014) was used to process the data. The stream isotope data for each site were plotted against the Global Meteoric Water Line (GMWL). The Local Meteoric Water Line (LMWL) was determined using a regression on precipitation samples from the complete BB dataset, which encompasses 2 May 2012 to 21 August 2015. From this, the line conditioned excess (lc-excess) was calculated as an indicator of fractionation. This defines the offset between the LMWL and stream water samples (Landwehr and Coplen, 2006) and is used to determine how the isotope values of stream waters differ from their presumed source (Landwehr and Coplen, 2006). Lc-excess was calculated using the following equation:

$$[1]\ \text{lc-excess} = \delta D - a * \delta^{18}O - b$$

where a and b are coefficients of the LMWL and δD and $\delta^{18}O$ are the isotopic composition of the stream water sample (‰).

Considering only 10 random DOC samples were analyzed per month, for each of the three sites, a multi-linear regression (MRL) was applied to derive a one year time series of daily DOC values. The regressions were based on temperature and discharge measurements from each of the catchments before kriging the results to the measured DOC values. For HW1 and the BB, when DOC derived from the FDOM probes was available, we used the value measured at 14:00 (the time at which DOC samples were autosampled) as the daily value. Where this data was not available, resulting data points from the MLR and kriging were used. Kruskal-Wallis tests were applied to test for statistically significant differences ($p < 0.05$) of DOC and isotope values between the catchments before applying a post-hoc test.

The FDOM data were initially filtered using the robfilter package (Fried et al., 2012) to remove anomalies caused for example by leaves blocking the sensor or from the removal of the sondes from the stream for inspection. Data from the EXO2 sonde at HW1 was then corrected for turbidity, temperature and inner filter effect using the method described by Downing et al.(2012). Turbidity was low in HW1 throughout the study, with an average value of 0.65 FNU, similar to that measured previously in the BB (Tunaley et al., 2016). Following the corrections, FDOM was converted to DOC, using the strong relationship between in-situ FDOM and laboratory analyzed DOC concentration from 57 data points, which covered both high and low flow conditions (r^2 = 0.95, p < 0.0001) (Figure S1, supplementary material). In order to compare the HW1 and the BB FDOM data, which were measured on different probes, a period of overlap between the EXO2 sonde and the TriOS sonde was undertaken. The period of comparison revealed the temporal dynamics were the same between both probes. However, the TriOS probe over-estimated the FDOM values and hence, overestimated the calculated DOC concentrations. Furthermore, the period of overlap was undertaken during winter when DOC concentrations were low. To overcome this problem, we used an already established FDOM – DOC relationship from a previous study in the BB when the EXO2 probe was monitoring for 1.5 years (Tunaley et al., 2016) to predict the FDOM values on dates when we had discrete DOC samples for the study period. Following this, we developed a relationship between the predicted FDOM versus FDOM measured from the TriOS probe (r^2 = 0.9, p < 0.0001) and corrected the TriOS data using the following equation:

$$[2]\ FDOM_{EXO2} = 10^{((0.0087 * FDOM_{TriOS}) + 1.1029)}$$

where $FDOM_{TriOS}$ is the value measured from the TriOS sensor. This was converted to DOC using the established FDOM-DOC relationship from the period when the EXO2 probe was in BB, using 244 points (r^2 = 0.74 p = < 0.0001) (Figure S2, supplementary material).

Twelve events were captured and extracted from the high frequency data at HW1 and the BB. An event was defined as an increase in discharge of more than 0.015 mm 15 min^{-1}. Hysteresis loops were plotted for each event, and the percentage increase in discharge and DOC, the lag time between peak discharge and peak DOC and the hysteresis index (HI) were calculated. The HI, which defines the shape and size of hysteresis loops, was defined using the method developed by Lloyd et al. (2016). Initially the discharge and DOC values were normalized for each event using the following equations:

$$[3]\ Normalised\ Q_t = \frac{Q_t - Q_{min}}{Q_{max} - Q_{min}}$$

$$[4]\ Normalised\ DOC_t = \frac{DOC_t - DOC_{min}}{DOC_{max} - DOC_{min}}$$

where Q_t and DOC_t are the discharge and DOC concentrations at time step *t*, $Q_{min}$and DOC_{min} are the minimum discharge and DOC values measured during the event, and $Q_{max}$and DOC_{max} are the maximum discharge and DOC values measured during the event. Following this, the HI was calculated as the difference between normalized DOC values on the rising and falling limb of an event at every 5 % interval of normalized discharge using the following equation:

$$[5]\ HI_{Qt} = DOC_{RL\_Qt} - DOC_{FL\_Qt}$$

where HI_{Qt} is the index at percentile *t* of discharge, DOC_{RL_Qt} is the DOC concentration on the rising limb at percentile *t* of discharge and DOC_{FL_Qt} is the DOC concentration on the falling limb at percentile *t* of discharge. This resulted in 19 values across the flow range, and the HI for each event is the mean of these. During some events discharge did not fully return to baseflow before the next event. When this happened the number of values available were used to calculate the mean (minimum was 16 values). The resulting values range between -1 and 1,

where the larger the absolute value, the wider the loop. The sign shows if an event displays clockwise or anticlockwise hysteresis. This method was developed from a previous method by Lawler et al. (2006); however, it eliminates the effect of differing pre-event concentrations on the index.

4. Results

4.1 Dynamics of stable isotopes and runoff generation

Throughout the study, precipitation mostly occurred as frequent, low intensity rainfall events. Sampling began in average summer conditions prior to a wet August 2014 (rainfall 280 % of the 1971 – 2000 average, see Hannaford et al. (2014). Following below average rainfall in September, the wettest conditions of the study period occurred in October and November, with precipitation values 175 % and 148 % of the 1971-2000 average, respectively (Hannaford et al., 2014; Parry et al., 2014). The highest daily precipitation occurred on 7 October 2014, when 41.2 mm (in the BB) fell. Accordingly, highest daily flows occurred on 8 October 2014 with 21.3 mm d^{-1} and 18.5 mm d^{-1} in HW1 and BB, respectively (Figure 2). Highest daily flow (26.6 mm d^{-1}) in the GIR in contrast, was recorded on 14 November 2014, in response to a 32.8 mm event, following a succession of smaller events (Figure 2). This November event also corresponded with the highest instantaneous (15 minute) discharge in all catchments (HW1 = 0.36 mm $15min^{-1}$, BB = 0.29 mm $15min^{-1}$ and GIR = 1.11 mm $15min^{-1}$). Thereafter, winter (December – February) and spring (March – May) approximated mean rainfall and average temperatures of 2.3°C and 5.8 °C, respectively. June 2015 was a dry period preceding a wet July 2015 when precipitation was 196 % of the 1971-2000 monthly average (Parry et al., 2015).

Figure 2 shows comparisons of the flows for the nested catchments based on 1 year of data. Median (Q_{50}), high (Q_1) and low (Q_{95}) flows were calculated for each of the catchments (Table 2). The headwater catchment (HW1) had the smallest high flows (Q_1 = 11.97 mm d^1) and largest low flows (Q_{95} = 0.35 mm d^{-1}) reflected in the flattest flow duration curve (inset of Figure 2). The GIR had the largest peak flows (Q_1 = 17.42 mm d^1) and smallest low flows (Q_{95} = 0.22 mm d^{-1}) producing the steepest flow duration curve of the catchments. The BB runoff response was intermediate in comparison. Flow regimes were characterised according to Botter et al. (2013) which uses the seasonal coefficient of variation of daily discharge (CV_Q) to discriminate between erratic ($CV_Q > 1.1$) and persistent regimes ($CV_Q < 0.9$) (Table 2). For all seasons, the GIR was the most erratic reflecting its flashy discharge regime compared to the more damped HW1 and the BB. The latter catchments were defined as erratic during summer (CV_Q = 1.5) and autumn (CV_Q = 1.4, CV_Q = 1.2, respectively) while persistent in spring (CV_Q = 0.5, CV_Q = 0.6, respectively) and winter (CV_Q = 0.6, CV_Q = 0.5, respectively) due to high base flows.

The δ^2H signature in precipitation showed high variability (ranging from -145.9 ‰ to -12.3 ‰, CV = 48 %) with more enriched values in summer (June - August mean = -49.2 ‰) and depleted values in winter (December – February: mean = -58.1 ‰) (Figure 3b, Table 3). This variability reflects the influence of seasonal temperature variation on equilibrium fractionation. Stream water δ^2H signatures from HW1, the BB and the GIR exhibited marked damping, ranging from -70.3 ‰ to -48.0 ‰, -72.2 ‰ to 50.9 ‰ and -81.8 ‰ to -50.6 ‰, respectively (Figure 3c). There were significant differences in the stream water isotope response between the catchments ($p < 0.05$). The most depleted δ^2H occurred during events, with all catchments measuring their most depleted values on 8 October in response to the highest precipitation event. The GIR measured the most depleted value (-81.8 ‰) whilst HW1 measured the least

depleted value during this event (-70.3 ‰). Overall, during events, the GIR stream water signal most reflected the isotope signature of precipitation with lower damping, consistent with quicker transformation of precipitation input into streams and lower mixing at that scale (Birkel et al., 2011). Upstream, the BB and HW1 displayed a more damped response. HW1 had the most enriched mean δ^2H in stream water, -56.8 ‰, compared to 58.1 ‰ and 59.1 ‰ for the BB and GIR, respectively (Table 3). The most enriched δ^2H sample (- 48 ‰) was from HW1 on 17 May 2014.

The difference between HW1 and the other sites was most pronounced in the summer months ($p < 0.001$), when stream isotopes were enriched. During the winter, the inter-site difference reduced and there was no significant difference between the catchments ($p > 0.05$). This summer enrichment resulted in HW1 having the most variability in δ^2H in stream water (CV = 6.6). The BB had the least variability (5.3 %) consistent with greater mixing and limited fractionation at this site.

Surface water isotope signatures for the catchments were plotted in dual isotope space (Figure 4). The LMWL had a slope of 7.6, an intercept of 4.1 ‰ and is close to the GMWL. It is evident for all sites that surface waters were occasionally enriched, deviating from the LMWL, but this was particularly evident at HW1. In summer, the local evaporation line (LEL) had a slope of 6.5 and an intercept of 4.6 ‰ for HW1, 6.0 and 7.7 ‰ for the BB, and 7.1 and 0.2 ‰ for the GIR. The lc-excess was also calculated to determine the offset between the LMWL and stream water (Landwehr and Coplen, 2006). This differs from the more widely applied deuterium-excess (d-excess, Dansgaard [1964]), which calculates the offset between the GMWL and stream water. However, here the LWML was used as a reference because it takes account of

the physical processes that may affect the isotopic composition of precipitation at the catchment scale (Tappa et al., 2016). Negative values reveal waters likely fractionated by evaporation whilst positive lc-excesses may indicate waters originating from several sources including relatively newly evaporated moisture (Landwehr et al., 2014). Precipitation lc-excess (Figure 5a) exhibited seasonal variability with more positive, depleted values in winter (median = 5.1 ‰) and negative, enriched values in summer (median = -1.7 ‰). HW1 had a lower median lc-excess (1.2 ‰) compared to the BB (1.8 ‰) and the GIR (1.9 ‰, Table 3) and also a higher percentage of negative values (24 %) versus the BB (16 %) and the GIR (20%) which could be indicative of greater evaporative fractionation. In all sites, the stream lc-excess had similar seasonal variability to that of precipitation with lower lc-excesses during the summer months (median = 0.5 ‰, 1.8 ‰ and 1.2 ‰ for HW1, the BB and GIR, respectively) compared to winter (mean = 2.6 ‰, 2.8 ‰ and 3.6 ‰ for HW1, the BB and GIR, respectively) (Table 3, Figure 5, Figure 6). Inter-site comparisons showed that all sites had significantly different lc-excesses ($p < 0.05$) during both summer and winter. However during winter the difference between the lc-excess in HW1 and the BB reduces ($p < 0.001$ in summer to $p = 0.02$ in winter).

4.2 Daily DOC dynamics

Daily DOC dynamics significantly differed between the catchments ($p < 0.001$) (Table 4, Figure 7). HW1 had highest mean DOC concentration (9.4 mg l^{-1}) compared to the BB (4.9 mg l^{-1}) and GIR (6 mg l^{-1}) (Table 4). Similar spatial variation for annual DOC loads were calculated, which was highest for HW1 (5.3 g C m^{-2} yr^{-1}) compared to the BB (3.7 g C m^{-2} yr^{-1}) and GIR (4.8 g C m^{-2} yr^{-1}). In HW1, the concentration exceeded 5 % of the time (C_5) was 16.4 mg l^{-1}. This was higher than the BB and GIR, which had C_5 values of 8.7 mg l^{-1} and 12.1 mg l^{-1}, respectively (Figure 7). The concentration exceeded 95 % of the time (C_{95}), 5.2 mg l^{-1},

was also higher in HW1 than in BB and GIR (2.6 mg l^{-1} and 2.4 mg l^{-1} respectively). Although the DOC concentration exceedance curves showed more pronounced differences than the flow duration curves, the general patterns in DOC response and differences were similar to the discharge response. HW1 differed the most from the other catchments ($p < 0.001$), whilst between the BB and GIR differences were only significant during summer months ($p = 0.013$) and not winter (Figure 7b and c).

Table 4 compares measured DOC samples and the derived daily time series values based on multi-linear regression (MRL). The derived and measured DOC values were comparable for all sites. Figure 8 shows daily DOC concentrations for the three sites illustrating the temporal DOC dynamics. As expected, concentrations were highest in the summer and autumn when biological activity is high and flushing occurs after warmer and drier periods. Maximum daily DOC concentration in HW1 was 22.1 mg l^{-1}, on 28 July 2014, in response to a 12.8 mm rainfall event which produced a very small peak in discharge (0.7 mm d^{-1}) during a dry period. In the BB and the GIR, the maxima occurred 6 days later (3 August 2014), once the catchment had re-wetted in response to two rainfall events (23 mm and 14.8 mm in BB, 29 mm and 16.4 mm in the GIR), which led to peak discharge of 3.8 mm d^{-1} in BB and 6.3 mm d^{-1} in GIR. DOC concentration peaked at 11.5 mg l^{-1} and 20.1 mg l^{-1}, respectively. For all sites, the minimum DOC concentrations occurred during the winter period (Dec- Feb) as a result of temperature controls on DOC production. Differences between sites were less pronounced during the winter period.

4.3 High-frequency DOC dynamics

Figure 9 shows the 15 minute time series of DOC and discharge for HW1 and BB (6 March 2015 to 3 August 2015). These data were consistent with the daily DOC measurements, with HW1 having higher inferred DOC concentrations during both baseflow and events (mean = 9.6 mg l^{-1}, max = 19.9 mg l^{-1}, min = 5.0 mg l^{-1}) compared to the BB (mean = 4.6 mg l^{-1}, max=12.0 mg l^{-1}, min = 2.6 mg l^{-1}). It was evident that as temperatures increased during spring and summer, the difference between HW1 and the BB DOC levels widened. Additional insights from the high frequency data included identification of diel variations, especially during summer dry periods. A five day dry period in June was examined in more detail. In HW1, the amplitude of the diel cycle was ~ 35 % (SD = 6.42 %) of the initial (minimum) concentration; equivalent to a 2.9 mg l^{-1} increase. In BB, the diel variation was less pronounced: 8 % (SD = 1.25 %) change of initial concentrations, equivalent to a 0.3 mg l^{-1} increase. In HW1, the time of maximum DOC concentration ranged between 12:45 – 14:15 (mean = 12:54) and the time of minimum concentration varied from 05:00 – 06:30 (mean = 05:24). The almost opposite was seen in BB, with the time of peak DOC between 05:00 – 06:45 (mean = 05:48) and the time of minimum concentration between 16:00 – 19:30 (mean = 18:15). Furthermore, diel variability, especially in HW1, appears to increase as summer progresses and temperatures increase (Figure 9).

The high frequency data facilitated capture of details of 12 events during the study (see numbers in Figure 9c). Hysteresis loops were plotted for each event to compare differences in dynamics between HW1 and the BB (Figure 10). At HW1, DOC generally increased mostly on the falling limb of the hydrograph. Seven of the hysteresis loops showed slight dilution on the rising limb of the hydrograph (E1, E3, E5, E9, E10, E11, E12). In contrast, in BB, dilution occurred on the rising limb only in event 10, while otherwise DOC increased on the rising limb.

Hysteresis statistics quantified the differences in event response at each site (Table 5). The percentage increase in DOC was lower in HW1 during all events (on average 24% compared to 65% in the BB). However, pre-event and peak DOC concentrations were always higher in HW1. Peak discharges were higher in BB compared to HW1 during six events; however, this did not appear to influence the differences in DOC dynamics. All events apart from event 2 showed anticlockwise hysteresis in HW1 (hysteresis direction A in Table 5) with discharge peaking before DOC. Lag times varied between 15 minutes (event 2) and 17 hours (events 1 and 4), with an average of 8 hours. During event 2, clockwise hysteresis (hysteresis direction C in Table 5) was observed, with DOC peaking 15 minutes prior to the discharge peak. In BB, all events showed anticlockwise hysteresis. Lag times varied between 1 hour (event 11) and 34 hours (event 9) with an average lag time of 7 hours. The hysteresis indices (loop shape) were calculated for each event to produce a dimensionless description of hysteresis, independent of the pre-event concentration (Lloyd et al., 2016). The larger the absolute value the wider the loop. The HI values varied between -0.32 and -0.73 for HW1 and between -0.23 and -0.85 for BB. The overall mean HI was slighter higher (closer to -1) in HW1 (-0.52) compared to BB (-0.50). However, both the range and standard deviation were higher in the BB (SD = 0.22) compared to HW1 (SD = 0.14), showing that HW1 had a more consistent hysteresis response between events.

Temporally, the highest DOC percentage increase occurred during event 8 in HW1 (56 %) and event 9 (123 %) in BB. Event 8 occurred on 4 July 2015 after a dry period in June and coincided with the lowest antecedent flows 14 days prior to the event (Q_{14}). Event 9 occurred subsequently, once the catchment began to wet up, though antecedent conditions were still dry

relative to the other events. The peak DOC concentration for both sites occurred during the highest flows measured (during event 10). However, there was no significant relationship between peak discharge and peak DOC during events at both sites ($p > 0.5$). On the other hand, the correlation between the mean discharge 14 days prior to the event (Q_{14}) and DOC peak for HW1 and BB was much stronger with correlation coefficients of $\rho = -0.71$ ($p = 0.005$) and $\rho = -0.77$ ($p= 0.012$), respectively. Antecedent temperature 14 days prior to the event (T_{14}) had an even stronger correlation with peak DOC for both sites ($\rho = 0.9$, $p = < 0.001$). This emphasises the influence of antecedent conditions on DOC dynamics during events. Hysteresis loops can be narrower during events that occur in close succession of an earlier event, hence, HI decreases (Lloyd et al., 2016). This was seen between events 1 and 2; events 4 and 5; as well as events 8 and 9 occurring within 2, 3 and 40 hours of each other, respectively. It was also evident in BB between events 10 and 11 (occurring within 1 hour of each other) when the HI index decreased from - 0.85 to - 0.26. On the other hand, the HI increased between events 10 and 11 in HW1 from -0.52 to -0.73.

5. Discussion

5.1 How do riparian peatlands generate runoff and how does this propagate at larger scales?

The nested, combined flow and stream water isotope measurements allowed us to investigate both the spatial and temporal dynamics in runoff generation and the role of riparian peatlands. In HW1, the extensive riparian peatland with its organic rich soils, combined with the low topography and presence of depressions in the peatland riparian area, resulted in consistently high storage usually connected to the channel network. The filling and flushing of these depressions resulted in attenuated peaks and opportunities for rapid mixing, resulting in the flattest flow duration curve and a damped isotope signal. This is consistent with Kværner and

Kløve (2006) who compared catchments with different dominant landscape units, showing the most damped isotope signals and reduced runoff fluctuations were in the catchment with the highest percentage peatland. Other studies contradict this finding as debates remain as to whether peatlands increase or decrease peak flows (e.g. Evans et al., 1999; Holden, 2005, 2004). However, this is likely influenced by the environmental setting of the peatland, its structure and the level of degradation (Bullock and Acreman, 2003; Acreman and Holden, 2013). More subtle effects of riparian peatlands on internal catchment processes can be revealed by deviations from the LMWL (Levy et al., 2014). The low gradient of the LEL and negative lc-excess values in summer suggest evaporation fractionation in near-surface soil water and surface water pools of the riparian peatland of HW1. This is consistent with other peatland sites in northern regions, where enriched isotope signals in surface waters have been reported (Levy et al., 2014; Carrer et al., 2015). Furthermore, previous spatial studies of HW1 have revealed evaporative signals within the peatland drainage network (Blumstock et al., 2015; Lessels et al., 2016; Sprenger et al., 2017). These signals were most apparent during summer low flow periods when rainfall is minimal and radiation is higher. Previous spatial sampling of the peatland drainage network by Sprenger et al. (2017) showed average lc-excesses during the summer sampling campaign (August) of 0.08_± 3.61 ‰. Increased discharges in the peatland drainage network resulted in more positive lc-excess values, in other words, a reduction in the evaporation signal (Sprenger et al., 2017). It is important to note that we were sampling only at the outlet of HW1. Hence, to see this evaporation signal in the stream water during dry periods, the surface pools in the riparian peatland where evaporation is occurring must be connected to the stream network. This implies that during low flows a major source of runoff is the constant seepage of the upper soil horizons of the peatlands to the stream channel, contributing to the high baseflows seen in HW1. This agrees with Kværner and Kløve (2008) who found that stored water in peatlands was the dominant source of runoff during low

499 flows. During wetter periods, the lc-excess of the peatland drainage network becomes more
500 positive as the evaporation signal is obscured by younger overland flow from more recent
501 rainfall, causing the outlet signal to become more positive (Lessels et al., 2016; Sprenger et al.,
502 2017). In winter, evaporation fractionation is no longer evident due to reduced temperatures
503 resulting in the inhibition of evaporative fractionation resulting in less significant differences
504 between HW1 and BB. This highlights the use of high resolution isotope data to be able to
505 identify subtle changes in runoff generation processes between events and low flows (Kværner
506 and Kløve, 2006; Meredith et al., 2009; Schulte et al., 2011; Levy et al., 2014).

507

508 Upscaling to the BB, the percentage cover of riparian peatland with extensive pools decreases
509 and the effects of evaporative fractionation were less evident as the summer lc-excess became
510 significantly more positive than HW1. Previous studies within the BB have shown that
511 groundwater is a significant contribution of stream flow due to the extensive drift deposits
512 (Birkel et al., 2011; Soulsby et al., 2016) and this contribution increases along the river channel
513 towards the lower parts of the main stem (Blumstock et al., 2015). Spatial sampling by
514 Sprenger et al. (2017) of groundwater in the BB revealed a more positive median lc-excess of
515 4.5 ± 1.5 ‰ due to being recharged mainly by depleted winter precipitation (Soulsby et al.,
516 2015). This groundwater contribution resulted in the high baseflow measured in this study.
517 During events, groundwater mixes with a greater proportion of displaced soil waters from the
518 riparian area (van Huijgevoort et al., 2016). Larger events result in connecting the minerogenic
519 hillslope waters. Mixing results in low event water contributions and the damped isotope
520 response recorded at the outlet of the BB (Tetzlaff et al., 2014). Hence, the BB has significantly
521 higher lc-excess values than HW1. Surprisingly, the BB LEL had a lower slope than HW1,
522 though this is explained by the higher contribution of groundwaters that plot above the LMWL

(hence the more positive lc-excess), indicating that the LEL gradient alone is not an accurate indication of evaporation fractionation.

The most variable regime in terms of flow and isotope response occurred in the largest GIR catchment, with the smallest percentage of riparian peatland. The LEL was closest to the LMWL suggesting that the streamflow measured at the outlet of the GIR was more strongly influenced by the meteoric signal (Levy, 2014). This was further indicated by the lc-excess values, which in winter showed the most positive lc-excesses due to the dominance of depleted precipitation, whilst in summer were more negative due to enriched precipitation rather than evaporative fractionation. The dominant meteoric signal in the GIR was a result of the high coverage of responsive soils (including peaty gleys and thin regosols) throughout the catchment combined with lower groundwater storage (Tetzlaff et al., 2007; Birkel et al., 2011). During events, connectivity increases to these responsive soils causing the fast routing of precipitation and the lack of storage in riparian areas resulting in less mixing with pre-event waters (McGlynn et al., 1999; Rodgers et al., 2005).

The more significant differences between catchments during summer low flows were a result of the constant connectivity between the riparian peats and stream in HW1, whereas in the BB and GIR greater disconnection with such landscape units occurred. During wetter periods, the sites' isotope signatures became more homogeneous (Lessels et al., 2016); though at the largest scale, the meteoric signal from the GIR overrides the signal of evaporation from HW1 and the signal of groundwater from the BB. This was in agreement with previous studies that the catchment characteristics, rather than catchment size per se, are controlling the scaling runoff responses (McGuire et al., 2005; Jensco et al., 2009; Laudon et al., 2011).

5.2 How do these changes in water sources and pathways affect DOC dynamics in surface water at different spatio-temporal scales?

The consistently higher DOC concentrations in HW1 are consistent with many other studies which have reported that catchments with the highest percentage peatland have the highest DOC concentration (Dawson et al., 2011; Olefeldt et al., 2013; Singh et al., 2015; Walling et al., 2015). This agrees with spatial sampling within HW1 and BB by Lessels et al. (2016) that found concentrations of DOC within the peaty pools of HW1 can be as high as 50 mg l^{-1} whereas BB soil waters tend to have lower concentrations (10-30 mg l^{-1}). The higher concentrations in HW1 were particularly noticeable during low flow conditions, consistent with findings by Laudon et al. (2011). The constant connection between the riparian peatland pools and the stream network during low flows, as highlighted by the lc-excess results, ensures a steady supply of DOC-rich water.

A temperature control on the DOC supply (Bonnett et al., 2006; Dawson et al., 2011) in HW1 was evident from the high-frequency data as differences between HW1 and the BB increased when progressing from spring to summer and the temperature increased. From the high-frequency data, it was also evident that diel variability occurred during low flows in both HW1 and the BB. Diel variation in DOC has been observed in previous studies (Spencer et al., 2007; Worrall et al., 2015), whilst others have noted an absence (Dawson et al., 2001). The majority of studies that reported diel dynamics have shown the peaks in DOC occurring at night or early in the morning, due to instream photic breakdown of DOC or the biological uptake during the day (Spencer et al., 2007; Worrall et al., 2015). Results from the BB also showed this behaviour, whereas, in HW1 the peak in DOC occurred around midday. Other studies have found similar results and suggest this is caused by heterotrophic organisms consuming DOC at

night in the absence of photosynthesis (Kaplan and Bott, 1982; Nimick et al., 2011). However, it is questionable why this could be happening in HW1 and the opposite in the BB when the catchments are in such close proximity to each other. Furthermore, previous studies usually reported diel variation of around 0.2 mg l^{-1} (Spencer et al., 2007), whereas, in HW1 the variability is ten times this amount. Investigation of diel discharge dynamics in HW1 revealed variability in phase with DOC dynamics, with maxima in the afternoon. Schwab et al. (2016) found similar discharge cycles during periods when vegetation was in dormant state and suggested this was caused by diel water temperature fluctuations in the upper layer of the riparian zone. These diel temperature fluctuations decrease water viscosity and hence increase hydraulic conductivity resulting in the increase of DOC rich inflows from the riparian peatland during the afternoon (Schwab et al. 2016). Schwab et al. (2016) found in a forested catchment the timings of the discharge diel cycle changed during the growing season as evapotranspiration became the dominant control. The period when diel variability was observed in HW1 was in the growing season (June), however in HW1 the viscosity control could still potentially be dominant due to the low percentage of forestry and hence evapotranspiration. Although further work is required, the data presented here shows that spatial differences in DOC dynamics may occur on frequencies missed using coarser sampling, highlighting the benefits of high-frequency measurements to fully understand catchment dynamics.

The high-frequency data also allowed us to capture 12 events throughout the study period to aid our understanding of the influence of riparian peatlands on DOC dynamics during high flows. A striking feature was that DOC in HW1 did not usually increase on the rising limb of the hydrograph and in some events a slight dilution was observed. One proposed mechanism is, considering the riparian peatland is constantly connected to the stream, that during events the initial increase in discharge includes a small amount of new water to dilute the connected

supply as it is displaced (Worrall et al., 2002; Grand-Clement et al., 2014). However, the effect was small and dilution was not as pronounced as reported for some other peatland catchments; for example, Laudon et al. (2011) observed dilution in DOC concentrations during snowmelt to ~ 60 % of baseflow values. The lower dilution in HW1 is probably due to it being offset by increasing hydrological connectivity to DOC sources further away from the stream, which were previously disconnected. With increased connectivity, hillslope water displaces DOC-rich water from the peatland pools. This was also apparent in the damping of the stream isotope response. As discharge decreases, the effect of dilution of the near stream sources diminishes but the increased connectivity results in the increase in DOC on the falling limb of the hydrograph. It is this connectivity to more distant, previously disconnected sources that can explain delayed DOC peaks and anticlockwise hysteresis (Inamdar et al., 2004; Pellerin et al., 2011; Tunaley et al., 2016). The DOC peaks were highest in HW1 due to the relative size of the riparian peat compared to the adjacent hillslope (Jensco et al., 2010) and thus greater supply.

The disproportional increase of DOC during small events following dry conditions, compared to large events with wet antecedent conditions, has been well documented (Oswald and Branfireun, 2014; Tunaley et al., 2016). It was evident from the strong relationships with Q_{14} and T_{14} that antecedent conditions were affecting event response in both HW1 and the BB. However, there appeared to be a stronger influence of dry antecedent conditions in HW1. Both the daily maximum DOC concentration and the maximum 15 minute DOC percentage increase occurred in response to very small events during dry periods. In contrast, in the other catchments the peaks occurred a few days later, once the catchments had wet up slightly. The following mechanism might explain the proportionally higher DOC caused by very small discharge events in HW1: here, the DOC supply is closer to the stream compared to the other catchments and even small discharge increases connect and displace DOC rich waters which

621 dominate event runoff. In BB and GIR, the DOC sources are less well connected and therefore
622 require larger events to re-connect to the stream (Mei et al., 2012). This is similar to Wallin et
623 al. (2015) who compared peatland and mineral soil dominated catchments and found the effect
624 of dry antecedent conditions greater for the peatland site.

625

626 A further difference to note is the recovery of DOC between successive events. The HI
627 decreased between events, which can be explained by the DOC concentrations not returning to
628 pre-event concentrations before the next event (Lloyd et al., 2016b). This appears to be the case
629 for most events that occurred within close proximity. However, after the largest event of the
630 high-frequency study period (event 10) concentrations returned to pre-event values and for the
631 next event, occurring 1 hour later, the HI decreased in the BB but not HW1. This could be due
632 to the DOC sources in close proximity to the stream in the BB being supply limited and being
633 already flushed (Lloyd et al., 2016b), which is indicative of a lower supply limitation and a
634 larger, more connected, store in HW1 (McGlynn and McDonnell, 2003; Morel et al., 2009).

635

636 As we upscaled to larger catchments and the percentage of riparian peatland decreased, the
637 baseflow DOC concentrations were significantly lower than HW1. This compliments previous
638 work by Laudon et al. (2011) that suggested such declining DOC concentrations were caused
639 by increased groundwater contributions at larger scales. Isotope results and previous studies
640 within BB suggest a high groundwater influence being the reason for low DOC concentrations
641 during low flows (Birkel et al. 2011; Lessels et al. 2015). A previous study by Tunaley et al.
642 (2016) in the BB found that during prolonged dry periods, the stream DOC approached its
643 minimum concentrations of the year (1 to 2 mg l^{-1}) whilst specific conductivity increased, indicating
644 the dominance of deeper groundwater. Furthermore, whilst HW1 remains connected to the near

stream peatland during baseflow, BB only has a small percentage still connected with a stream signal more diluted by this groundwater. Any viscosity fluctuation effect on diel DOC was not evident in BB likely due to the groundwater domination during low flows. Hence instream processes are most likely the dominant control on diel DOC dynamics in BB. Upscaling further to the GIR, we know from the isotope results and previous studies that the GW contribution decreases, however, the baseflow DOC also decreased at this scale. This decrease in baseflow DOC could be explained by reduced connectivity to DOC sources at low flows.

During the highest flows, responses were more similar between the catchments, consistent with greater connectivity to DOC rich sources, resulting in anticlockwise hysteresis loops. However, unlike HW1, DOC in BB generally increased on the rising limb of the hydrograph and did not display signs of dilution. The relatively larger disconnection between the stream and DOC sources during low flows in the BB resulted in a higher percentage increase in DOC during events, as DOC source areas previously disconnected become connected. This is consistent with Singh et al. (2015) who showed that the percentage increase in event DOC was highest in the larger catchments, although DOC concentration peaks were higher in smaller wetland dominated streams. Limited high-frequency data was available for the GIR. However, the daily data showed that at this larger scale, even though the proportion of riparian peat decreased, daily DOC peaks during high flows were higher than BB and similar to peaks in HW1. This is explained by high coverage of peaty gleys and peaty podzols which results in the flashy runoff in the GIR. The higher percentage of organic soils (peaty podsols, humic iron podsols and peaty rankers), which are not classified as peat, in the GIR means that during events, when these soils become connected, flushes of DOC are greater. Whereas during particularly high flows, higher connectivity to minerogenic soils (brown rankers) in the upper hillslopes in the BB dilutes not only the evaporation signal but also DOC concentrations in the stream (Tunaley et al., 2016).

Figure 11 synthesises the spatio-temporal variability of processes controlling isotope and DOC signals at the outlets of the three catchment scales. Overall, the key control on DOC mobilisation as we upscaled were the connections and disconnections of the dominant runoff contributing areas (McGlynn and McDonnell, 2003; Burt, 2005; Olefeldt et al., 2013).

6. Wider Implications

Peatlands in catchment headwaters are currently the focus for environmental management initiatives in parts of the UK and elsewhere. In many parts of the UK, peatlands have been degraded and significantly altered through burning, drainage for agriculture and afforestation (Holden et al., 2004; Grand-Clement et al., 2014). However, the more recent recognition of the ecosystem services provided by peatlands has highlighted the potential benefits of restoration targeted at attenuating flooding, through increased water storage, and in reducing carbon losses, which can cause high DOC concentrations in drainage from degraded peat (Bragg, 2002; Wilson et al., 2011; Parry et al., 2014). Whilst many such projects are relatively small scale, the results presented here suggest that the effects of processes occurring in riparian peatlands are moderated at larger scales as other landscape elements become the dominant contributors of runoff (Acreman and Holden, 2013). This has implications for theplanning and promotion of peatland restoration projects, especially those that occur in small scale upland areas where the downstream propagation of benefits may be difficult to detect. The study highlights the need for research not only into the processes occurring in the peatlands alone (Bullock and Acreman, 2003) but the integration of this into larger scale understanding of landscape hydrology, to understand the downstream benefits of restoration schemes in terms of the management of water quantity and quality.

7. Conclusions

We examined the impact of riparian peatlands on isotopes in runoff to infer flow paths and understand stream water DOC dynamics across a range of hydrologic conditions and spatio-temporal scales. Daily stable isotope data allowed us to identify dynamics in dominant runoff sources and flowpaths. Results indicated that riparian peatlands significantly alter the runoff response and impact diel, event and seasonal DOC dynamics. These dynamics are driven by the degree of connectivity between DOC sources and the stream network. As scale increases, and the percentage of riparian peatland decreases, the disconnection between landscape units and streams became more pronounced. Across all three scales, the main drivers of DOC mobilisation were the connections and disconnections of the dominant runoff contributing areas. Overall, our study highlights the usefulness of linking isotope tracers with DOC, particularly high frequency DOC, to improve our knowledge of how hydrological connectivity and runoff generation processes influence the amount of DOC delivered to the stream.

Acknowledgments

The authors would like to thank the European Research Council ERC (project GA 335910 VeWa) for funding the VeWa project. Part of this work was funded through the Natural Environment Research Council (NERC) (project NE/K000268/1). We would also like to thank our NRI colleagues for all their help with field and laboratory work, especially Jason Lessels, Matthias Sprenger, Jonathan Dick, Audrey Innes and Ann Porter. We would like to also thank Iain Malcolm (Marine Scotland Science) for providing AWS and Girnock flow data. Please contact the authors for access to the data used in this paper.

References

718 Acreman, M., Holden, J., 2013. How wetlands affect floods. Wetlands. 33, 773–786.
719 doi:10.1007/s13157-013-0473-2

720 Aitkenhead, J.A., Hope, D., Billett, M.F., 1999. The relationship between dissolved organic carbon in
721 stream water and soil organic carbon pools at different spatial scales. Hydrol. Process.13, 1289–
722 1302, doi:10.1002/(SICI)1099-1085(19990615)13:8<1289::AID-HYP766>3.0.CO;2-M

723 Ali, G., Birkel, C., Tetzlaff, D., Soulsby, C., Mcdonnell, J.J., Tarolli, P., 2014. A comparison of wetness
724 indices for the prediction of observed connected saturated areas under contrasting conditions. Earth
725 Surf. Process. Landforms 39, 399–413. doi:10.1002/esp.3506

726 Allan, C.J., Vidon, P., Lowrance, R., 2008. Frontiers in riparian zone research in the 21st century.
727 Hydrol. Process. 22, 3221–3222. doi:10.1002/hyp.7086

728 Billett, M.F., Cresser, M.S., 1992. Predicting stream-water quality using catchment and soil chemical
729 characteristics. Environ. Pollut. 77, 263–268. doi:10.1016/0269-7491(92)90085-O

730 Birkel, C., Soulsby, C., Tetzlaff, D., 2014. Integrating parsimonious models of hydrological
731 connectivity and soil biogeochemistry to simulate stream DOC dynamics. Biogeosciences. 119,
732 1030-1047. doi:10.1002/2013JG002551

733 Birkel, C., Soulsby, C., Tetzlaff, D., 2011. Modelling catchment-scale water storage dynamics:
734 Reconciling dynamic storage with tracer-inferred passive storage. Hydrol. Process. 25, 3924–3936.
735 doi:10.1002/hyp.8201

736 Blöschl, G., 2001. Scaling in hydrology. Hydrol. Process. 15, 709–711. doi:10.1002/hyp.432

737 Blumstock, M., Tetzlaff, D., Malcolm, I.A., Nuetzmann, G., Soulsby, C., 2015. Baseflow dynamics:
738 Multi-tracer surveys to assess variable groundwater contributions to montane streams under low
739 flows. J. Hydrol. 527, 1021–1033. doi: 10.1016/j.jhydrol.2015.05.019

740 Bonnett, S.A.F., Ostle, N., Freeman, C., 2006. Seasonal variations in decomposition processes in a
741 valley-bottom riparian peatland. Sci. Total Environ. 370, 561–573.
742 doi:10.1016/j.scitotenv.2006.08.032

743 Botter, G., Basso, S., Rodriguez-Iturbe, I., Rinaldo, A., 2013. Resilience of river flow regimes. Proc.
744 Natl. Acad. Sci. 110, 12925-12930. doi: 10.1073/pnas.1311920110

745 Bragg, O.M., 2002. Hydrology of peat-forming wetlands in Scotland. Sci. Total Environ. 294, 111–
746 129. doi:10.1016/S0048-9697(02)00059-1

747 Bullock, A., Acreman, M., 2003. The role of wetlands in the hydrological cycle. Hydrol. Earth Syst.
748 Sci. 7, 358–389. doi:10.5194/hess-7-358-2003

749 Burt, T.P., 2005. A third paradox in catchment hydrology and biogeochemistry: Decoupling in the
750 riparian zone. Hydrol. Process. 19, 2087–2089. doi:10.1002/hyp.5904

751 Buttle, J.M., Peters, D.L., 1997. Inferring hydrological processes in a temperate basin using isotopic
752 and geochemical hydrograph separation. Hydrol. Process. 11, 557–573. doi: 10.1002/(SICI)1099-
753 1085(199705)11:6<557::AID-HYP477>3.0.CO;2-Y

754 Capell, R., Tetzlaff, D., Malcolm, I. A., Hartley, A.J., Soulsby, C., 2011. Using hydrochemical tracers
755 to conceptualise hydrological function in a larger scale catchment draining contrasting geologic
756 provinces. J. Hydrol. 408, 164–177. doi:10.1016/j.jhydrol.2011.07.034

757 Carrer, G.E., Rousseau, A.N., Jutras, S., Fossey, M., 2015. Assessment of the impact of pools on the
758 water isotopic signature of a boreal patterned peatland. Hydrol. Process. 30, 1292–1307.
759 doi:10.1002/hyp.10715

760 Dansgaard, W., 1964. Stable isotopes in precipitation. Tellus. 16, 436-468. doi: 10.1111/j.2153-
761 3490.1964.tb00181.x.

762 Dawson, J.J.C., Billett, M.F., Hope, D., 2001. Diurnal variations in the carbon chemistry of two acidic
763 peatland streams in north-east Scotland. Freshw. Biol. 46, 1309–1322. doi: 10.1046/j.1365-
764 2427.2001.00751.x

765 Dawson, J.J.C., Tetzlaff, D., Speed, M., Hrachowitz, M., Soulsby, C., 2011. Seasonal controls on DOC
766 dynamics in nested upland catchments in NE Scotland. Hydrol. Process. 25, 1647–1658.
767 doi:10.1002/hyp.7925

768 Dick, J.J., Tetzlaff, D., Birkel, C., Soulsby, C., 2015. Modelling landscape controls on dissolved organic
769 carbon sources and fluxes to streams. Biogeochemistry 122, 361–374. doi:10.1007/s10533-014-
770 0046-3

771 Downing, B.D., Pellerin, B. A., Bergamaschi, B. A., Saraceno, J.F., Kraus, T.E.C., 2012. Seeing the
772 light: The effects of particles, dissolved materials, and temperature on in situ measurements of DOM
773 fluorescence in rivers and streams. Limnol. Oceanogr. Methods 10, 767–775.
774 doi:10.4319/lom.2012.10.767

775 Evans, M.G., Burt, T.P., Holden, J., Adamson, J.K. 1999. Runoff generation and water table
776 fluctuations in blanket peat: Evidence from UK data spanning the dry summer of 1995. J. Hydrol.
777 221, 141-160. doi: 10.1016/S0022-1694(99)00085-2

778 Fried, R., Schettlinger,K., Borowski, M., 2012. robfilter: R package version 4.0. doi: http://CRAN.R-
779 project.org/package=robfilter

780 Geris, J., Tetzlaff, D., McDonnell, J., Soulsby, C., 2014. The relative role of soil type and tree cover on
781 water storage and transmission in northern headwater catchments. Hydrol. Process. 29, 1844–1860.
782 doi:10.1002/hyp.10289

783 Gorham, E., 1991. Northern Peatlands : Role in the Carbon Cycle and Probable Responses to Climatic
784 Warming. Ecol. Appliations. 1, 182–195. doi: 10.2307/1941811

785 Grabs, T., Bishop, K., Laudon, H., Lyon, S.W., Seibert, J., 2012. Riparian zone hydrology and soil
786 water total organic carbon (TOC): Implications for spatial variability and upscaling of lateral riparian
787 TOC exports. Biogeosciences 9, 3901–3916. doi:10.5194/bg-9-3901-2012

788 Grand-Clement, E., Luscombe, D., Anderson, K., Gatis, N., Benaud, P., Brazier R., 2014. Antecedent
789 conditions control carbon loss and downstream water quality from shallow, damaged peatlands. Sci.
790 Total Environ. 493, 961-973. doi: 10.1016/j.scitotenv.2014.06.091

791 Haapalehto, T., Kotiaho, J.S., Matilainen, R., Tahvanainen, T., 2014. The effects of long-term drainage
792 and subsequent restoration on water table level and pore water chemistry in boreal peatlands. J.
793 Hydrol. 519, 1493–1505. doi:10.1016/j.jhydrol.2014.09.013

794 Hannaford, J., Muchan, K., Lewis, M., Clemas, S., 2014. Hydrological Summary for the United
795 Kingdom: August 2014. NERC Open Research Archive (NORA). Available at:
796 http://nora.nerc.ac.uk

797 Holden, J., 2005. Peatland hydrology and carbon release: why small-scale process matters. Philos.
798 Trans. R. Soc. A Math. Phys. Eng. Sci. 363, 2891–2913. doi:10.1098/rsta.2005.1671

799 Holden, J., 2004. Artificial drainage of peatlands: hydrological and hydrochemical process and wetland
800 restoration. Prog 28, 95–123. doi:10.1191/0309133304pp403ra

801 Hope, D., Billett, M.F., Cresser, M.S., 1997. Exports of organic carbon in two river systems in NE
802 Scotland. J. Hydrol. 193, 61–82. doi:10.1016/S0022-1694(96)03150-2

803 Hrachowitz, M., Soulsby, C., Tetzlaff, D., Speed, M., 2010. Catchment transit times and landscape
804 controls-does scale matter? Hydrol. Process. 24, 117–125. doi:10.1002/hyp.7510

805 Inamdar, S. P., Christopher, S.F., Mitchell, M.J., 2004. Export mechanisms for dissolved organic
806 carbon and nitrate during summer storm events in a glaciated forested catchment in New York,
807 USA, Hydrol. Process. 18, 2651–2661. doi:10.1002/hyp.5572
808

809 Inamdar, S., Singh, S., Dutta, S., Levia, D., Mitchell, M., Scott, D., Bais, H., McHale, P., 2011.
810 Fluorescence characteristics and sources of dissolved organic matter for stream water during storm
811 events in a forested mid-Atlantic watershed. J. Geophys. Res. Biogeosciences 116, G03043.
812 doi:10.1029/2011JG001735

813 Jencso, K.G., McGlynn, B.L., Gooseff, M.N., Bencala, K.E., Wondzell, S.M., 2010. Hillslope
814 hydrologic connectivity controls riparian groundwater turnover: Implications of catchment structure
815 for riparian buffering and stream water sources. Water Resour. Res. 46, 1–18.
816 doi:10.1029/2009WR008818

817 Kaplan, L.A., Bott, T.L., 1982. Diel fluctuations of DOC generated by algae in a piedmont stream.
818 Limno. Oceanog. 27, 1091-1100. doi: 10.4319/lo.1982.27.6.1091

819 Kirchner, J.W., Feng, X., Neal, C., Robson, A.J., 2004. The fine structure of water-quality dynamics:
820 the (high-frequency) wave of the future. Hydrol. Process. 18, 1353–1359. doi:10.1002/hyp.5537

821 Kværner, J., Kløve, B., 2008. Generation and regulation of summer runoff in a boreal flat fen. J. Hydrol.
822 360, 15–30. doi:10.1016/j.jhydrol.2008.07.009

823 Kværner, J., Kløve, B., 2006. Tracing sources of summer streamflow in boreal headwaters using
824 isotopic signatures and water geochemical components. J. Hydrol. 331, 186–204.
825 doi:10.1016/j.jhydrol.2006.05.008

826 Landwehr, J.M., Coplen, T.B., 2006. Line-conditioned excess: a new method for characterizing stable
827 hydrogen and oxygen isotope ratios in hydrologic systems. In Isotopes in Environmental Studies,
828 Aquatic Forum 2004, IAEA–CSP–26. International Atomic Energy Agency: Vienna, 132–135.

829 Landwehr, J.M., Coplen, T.B., Stewart, D.W., 2014. Spatial, seasonal, and source variability in the
830 stable oxygen and hydrogen isotopic composition of tap waters throughout the USA. Hydrol.
831 Process. 28, 5382–5422. doi:10.1002/hyp.10004

832 Laudon, H., Berggren, M., Ågren, A., Buffam, I., Bishop, K., Grabs, T., Jansson, M., Köhler, S., 2011.
833 Patterns and Dynamics of Dissolved Organic Carbon (DOC) in Boreal Streams: The Role of
834 Processes, Connectivity, and Scaling. Ecosystems 14, 880–893. doi:10.1007/s10021-011-9452-8

835 Laudon, H., Sjöblom, V., Buffam, I., Seibert, J., Mörth, M., 2007. The role of catchment scale and
836 landscape characteristics for runoff generation of boreal streams. J. Hydrol. 344, 198–209.
837 doi:10.1016/j.jhydrol.2007.07.010

838 Lawler, D.M., Petts, G.E., Foster, I.D.L., Harper, S., 2006. Turbidity dynamics during spring storm
839 events in an urban headwater river system: The Upper Tame, West Midlands, UK. Sci. Total
840 Environ. 360, 109–126. doi:10.1016/j.scitotenv.2005.08.032

841 Lessels, J.S., Tetzlaff, D., Birkel, C., Dick, J., Soulsby, C., 2016. Water sources andmixing in riparian
842 wetlands revealed by tracers and geospatial analysis. Water Resour. Res. 52, 456–470. doi:10.1002/
843 2015WR017519

844 Levy, Z.F., Siegel, D.I., Dasgupta, S.S., Glaser, P.H., Welker, J.M., 2014. Stable isotopes of water show
845 deep seasonal recharge in northern bogs and fens. Hydrol. Process. 28, 4938–4952.
846 doi:10.1002/hyp.9983

847 Lloyd, C.E.M., Freer, J.E., Johnes, P.J., Collins, A.L., 2016. Technical Note: Testing an improved index
848 for analysing storm discharge-concentration hysteresis. Hydrol. Earth Syst. Sci. 20, 625–632.
849 doi:10.5194/hess-20-625-2016

850 Lloyd, C.E.M., Freer, J.E., Johnes, P.J., Collins, A.L., 2016. Using hysteresis analysis of high-resolution
851 water quality monitoring data, including uncertainty, to infer controls on nutrient and sediment
852 transfer in catchments. Sci. Total Environ. 543, 338-404. doi: 10.1016/j.scitotenv.2015.11.028

853 McGlynn, B.L., McDonnell, J.J., 2003. Quantifying the relative contributions of riparian and hillslope
854 zones to catchment runoff. Water Resour. Res. 39, 1310. doi:10.1029/2003WR002091

McGlynn, B.L., McDonnell, J.J., Shanley, J.B., Kendall, C., 1999. Riparian zone flowpath dynamics during snowmelt in a small headwater catchment. J. Hydrol. 222, 75–92. doi:10.1016/S0022-1694(99)00102-X

McGuire,K.J., McDonnell, J,J., Weiler, M., Kendall, C., McGlynn, B.L., Welker,J.M., Seibert, J., 2005. The role of topography on catchment-scale water residence time. Water Resour. Res. 41, W05002. doi:10.1029/2004WR003657.

Mei, Y., Hornberger, G.M., Kaplan, L.A., Newbold, J.D., Aufdenkampe, A.K., 2012. Estimation of dissolved organic carbon contribution from hillslope soils to a headwater stream. Water Resour. Res. 48, 1–17. doi:10.1029/2011WR010815

Meredith, K.T., Hollins, S.E., Hughes, C.E., Cendón, D.I., Hankin, S., Stone, D.J.M., 2009. Temporal variation in stable isotopes (18O and 2H) and major ion concentrations within the Darling River between Bourke and Wilcannia due to variable flows, saline groundwater influx and evaporation. J. Hydrol. 378, 313–324. doi:10.1016/j.jhydrol.2009.09.036

Morel, B., Durand, P., Jaffrezic, A., Gruau, G., Molenat, J., 2009. Sources of dissolved organic carbon during stormflow in a headwater agricultural catchment. Hydrol. Process. 23, 2888–2901. doi:10.1002/hyp.7379

Nimick, D., Gammons, C., Parker, S., 2011. Diel biogeochemical processes and their effect on the aqueous chemistry of streams: A review. Chem.Geol. 283, 3-17. doi: 10.1016/j.chemgeo.2010.08.017

Olefeldt, D., Roulet, N., Giesler, R. and Persson, A., 2013. Total waterborne carbon export and DOC composition from ten nested subarctic peatland catchments—importance of peatland cover, groundwater influence, and inter-annual variability of precipitation patterns. Hydrol. Process. 27, 2280–2294. doi: 10.1002/hyp.9358

879 Oswald, C. J., and B. A. Branfireun, 2014. Antecedent moisture conditions control mercury and
880 dissolved organic carbon concentration dynamics in a boreal headwater catchment. Water Resour.
881 Res. 50, 6610–6627. doi:10.1002/2013WR014736

882 Parry, L. E., Holden, J., Chapman, P. J., 2014. Restoration of blanket peatlands. J. Environ. Manag.
883 133, 193–205. doi: 10.1016/j.jenvman.2013.11.033

884 Parry, S., Muchan, K., Lewis, M., Clemas, S., 2014. Hydrological Summary for the United Kingdom:
885 November 2014. NERC Open Research Archive (NORA). Available at: http://nora.nerc.ac.uk

886 Pellerin, B. A., Saraceno,J.F., Shanley, J. B., Sebestyen, S. D., Aiken, G.R., Wollheim,W.M.,
887 Bergamaschi, B. A., 2012. Taking the pulse of snowmelt: In situ sensors reveal seasonal, event and
888 diurnal patterns of nitrate and dissolved organic matter variability in an upland forest
889 stream. Biogeochemistry. 108, 183–198. doi:10.1007/s10533-011-9589-8
890

891 Ramchunder, S.J., Brown, L.E., Holden, J., 2009. Environmental effects of drainage, drain-blocking
892 and prescribed vegetation burning in UK upland peatlands. Prog. Phys. Geogr. 33, 49–79.
893 doi:10.1177/0309133309105245

894 Rodgers, P., Soulsby, C., Waldron, S., 2005. Stable isotope tracers as diagnostic tools in upscaling flow
895 path understanding and residence time estimates in a mountainous mesoscale catchment. Hydrol.
896 Process. 19, 2291–2307. doi:10.1002/hyp.5677

897 Saraceno, J.F., Pellerin, B. A., Downing, B.D., Boss, E., Bachand, P. a. M., Bergamaschi, B. a., 2009.
898 High-frequency in situ optical measurements during a storm event: Assessing relationships between
899 dissolved organic matter, sediment concentrations, and hydrologic processes. J. Geophys. Res. 114,
900 G00F09. doi:10.1029/2009JG000989

901 Schulte, P., van Geldern, R., Freitag, H., Karim, A., Négrel, P., Petelet-Giraud, E., Probst, A., Probst,
902 J.L., Telmer, K., Veizer, J., Barth, J.A.C., 2011. Applications of stable water and carbon isotopes in

903 watershed research: Weathering, carbon cycling, and water balances. Earth-Science Rev. 109, 20–
904 31. doi:10.1016/j.earscirev.2011.07.003

905 Siegel, D.I., Glaser, P., 2006. The Hydrology of Peatlands. Ecol. Stud. 188, 289–311. doi:10.1007/978-
906 3-540-31913-9_13

907 Singh, S., Inamdar, S., Mitchell, M., 2015. Changes in dissolved organic matter (DOM) amount and
908 composition along nested headwater stream locations during baseflow and stormflow. Hydrol.
909 Process. 29, 1505–1520. doi:10.1002/hyp.10286

910 Smart, R.P., Soulsby, C., Cresser, M., Wade, A. and Billett, M.F., 2001. Riparian zone influence on
911 stream water chemistry at different spatial scales: a GIS based approach. Sci. Total Environ. 280,
912 173-193.

913 Soulsby, C., Birkel, C., Geris, J., Dick, J., Tunaley, C., Tetzlaff, D., 2015. Stream water age distributions
914 controlled by storage dynamics and nonlinear hydrologic connectivity: Modeling with high-
915 resolution isotope data. Water Resour. Res. 51, 7759–7776. doi:10.1002/2015WR017888

916 Soulsby, C., Bradford, J., Dick, J., P. McNamara, J., Geris, J., Lessels, J., Blumstock, M., Tetzlaff, D.,
917 2016. Using geophysical surveys to test tracer-based storage estimates in headwater catchments.
918 Hydrol. Process. doi:10.1002/hyp.10889Soulsby, C., Malcolm, R, Helliwell, R.C., Ferrier, R.C., and
919 Jenkins, A. 2000. Isotope hydrology of the Allt a' Mharcaidh catchment, Cairngorm mountains,
920 Scotland: implications for hydrological pathways and water residence times. Hydrol. Process. 14,
921 747-762. doi: 10.1002/(SICI)1099-1085(200003)14:4<747::AID-HYP970>3.0.CO;2-0

922 Soulsby, C., Rodgers, P., Smart, R., Dawson, J., Dunn, S., 2003. A tracer-based assessment of
923 hydrological pathways at different spatial scales in a mesoscale Scottish catchment. Hydrol. Process.
924 17, 759–777. doi:10.1002/hyp.1163

925 Soulsby, C., Tetzlaff, D., Dunn, S.M., Waldron, S., 2006. Scaling up and out in runoff process
926 understanding : insights from nested experimental catchment studies. Hydrol. Process. 20, 2461–
927 2465. doi: 10.1002/hyp.6338

928 Spencer, R., Pellerin, B., Bergamaschi, B., Downing, B., Kraus, T., Smart, D., Dahlgren, R., Hernes,
929 P., 2007. Diurnal variability in riverine dissolved organic matter composition determined by in situ
930 optical measurement in the San Joaquin River (California , USA). Hydrol. Process. 21, 3181-3189.
931 doi: 10.1002/hyp.6887

932 Sprenger, M., Tetzlaff, D., Tunaley, C., Dick, J., Soulsby, C., 2017. Evaporation fractionation in a
933 peatland drainage network affects stream water isotope composition. Water Resour.Res. 53, doi:
934 10.1002/2016WR019258

935 Strohmeier, S., Knorr, K.-H., Reichert, M., Frei, S., Fleckenstein, J.H., Peiffer, S., Matzner, E., 2013.
936 Concentrations and fluxes of dissolved organic carbon in runoff from a forested catchment: insights
937 from high frequency measurements. Biogeosciences. 10, 905–916. doi:10.5194/bg-10-905-2013

938 Schwab, M., Klaus, J., Pfister, L., Weiler, M., 2016. Diel discharge cycles explained through viscosity
939 fluctuations in riparian inflow. Water Resour.Res. 52, 8744-8755. doi 10.1002/2016WR018626

940 Tappa, D. J., Kohn, M. J., McNamara, J. P., Benner, S. G., Flores, A. N., 2016. Isotopic composition
941 of precipitation in a topographically steep, seasonally snow-dominated watershed and implications
942 of variations from the global meteoric water line. Hydrol. Process. 30, 4582–4592.
943 doi: 10.1002/hyp.10940

944 Tetzlaff, D., Birkel, C., Dick, J., Geris, J., Soulsby, C., 2014. Storage dynamics in hydropedological
945 units control hillslope connectivity, runoff generation and the evolution of catchment transit time
946 distributions. Water Resour. Res. 50, 969-985. doi:10.1002/2013WR014147

947 Tetzlaff, D., Buttle, J., Carey, S.K., van Huijgevoort, M.H.J., Laudon, H., Mcnamara, J.P., Mitchell,
948 C.P.J., Spence, C., Gabor, R.S., Soulsby, C., 2015. A preliminary assessment of water partitioning
949 and ecohydrological coupling in northern headwaters using stable isotopes and conceptual runoff
950 models. Hydrol. Process. 29, 5153–5173. doi:10.1002/hyp.10515

951 Tetzlaff, D., Soulsby, C., Bacon, P.J., Youngson, A.F., 2007. Connectivity between landscapes and
952 riverscapes — a unifying theme in integrating hydrology and ecology in catchment science ? Hydrol.
953 Process. 21, 1385–1389. doi: 10.1002/hyp.6701

954 Tetzlaff, D., Soulsby, C., Waldron, S., Malcolm, I.A., Bacon, P.J., Dunn, S.M., Lilly, A., Youngson,
955 A.F., 2007. Conceptualization of runoff processes using a geographical information system and
956 tracers in a nested mesoscale catchment. Hydrol. Process. 21, 1289–1307. doi:10.1002/hyp.6309

957 Tunaley, C., Tetzlaff, D., Lessels, J., Soulsby, C., 2016. Linking high-frequency DOC dynamics to the
958 age of connected water sources. Water Resour. Res. doi:10.1002/2015WR018419

959 Tyler, J.J., Leng, M.J., Arrowsmith, C., 2007. Seasonality and the isotope hydrology of Lochnagar, a
960 Scottish mountain lake: implications for palaeoclimate research. The Holocene. 17, 717–727.
961 doi:10.1177/0959683607080513

962 Vidon, P., Allan, C., Burns, D., Duval, T.P., Gurwick, N., Inamdar, S., Lowrance, R., Okay, J., Scott,
963 D., Sebestyen, S., 2010. Hot spots and hot moments in riparian zones: Potential for improved water
964 quality management. J. Am. Water Resour. Assoc. 46, 278–298. doi:10.1111/j.1752-
965 1688.2010.00420.x

966 Wallin, M. B.,Weyhenmeyer, G.A., Bastviken, D., Chmiel, H.E., Peter, S., Sobek, S., Klemedtsson, L.,
967 2015. Temporal control on concentration, character, and export of dissolved organic carbon in two
968 hemiboreal headwater streams draining contrasting catchments, J. Geophys. Res. Biogeosci. 120,
969 832–846. doi:10.1002/ 2014JG002814

970 Wilson L, Wilson J, Holden J, Johnstone I, Armstrong A, Morris M., 2011. Ditch blocking, water
971 chemistry and organic carbon flux: evidence that blanket bog restoration reduces erosion and fluvial
972 carbon loss. Sci Total Environ, 409, 2010–2018. doi: 10.1016/j.scitotenv.2011.02.036

973 Wilson, H.F., Saiers, J.E., Raymond, P. a., Sobczak, W. V., 2013. Hydrologic Drivers and Seasonality
974 of Dissolved Organic Carbon Concentration, Nitrogen Content, Bioavailability, and Export in a
975 Forested New England Stream. Ecosystems. 16, 604–616. doi:10.1007/s10021-013-9635-6

976 Worrall, F., Burt, T.P., Jaetan, R.Y., Warburton, J., Shedden.R., 2002, Release of dissolved organic
977 carbon from upland peat, Hydrol. Processes, 16, 3487–3504. doi: 10.1002/hyp.1111

978 Worral, F., Howden, N.J.K., Burt,T.P., 2015. Understanding the diurnal cycle in fluvial dissolved
979 organic carbon – The interplay of in-stream residence time, day length and organic matter turnover.
980 J. Hydrol. 523, 830-838. doi: 10.1016/j.jhydrol.2015.01.075

981

982

983

984 **TABLES:**

985

Site	HW1	Bruntland Burn	Girnock
Area (km^2)	0.65	3.20	31.00
Topography			
Mean elevation (m)	339	351	405
Min elevation (m)	269	248	233
Max elevation (m)	518	539	852
Mean slope (°)	15	13	9
Bedrock geology			
Granite (%)	61	46	68
Metamorphic (%)	39	54	32
Soils			
Alluvial soils (%)			2
Brown ranker (%)	45	31	9
Humus-iron podsols (%)			24
Peat (%)	15	9	4
Peaty podsols/gleys (%)	20	48	57
Peaty ranker (%)	20	12	4
Riparian peat (%)	81	53	9
Land cover			
Heather moorland(%)	35	20	70
Peat bog(%)	15	13	4
Forestry (%)	25	34	8
Grassland (%)		4	12
Rock, boulder field (%)	24.8	29	6

986

987 **Table 1:** Summary of catchment characteristics of the three nested sites studied

988

Site	HW1	Bruntland Burn	Girnock
Q_1 (mm d^{-1})	11.97	13.98	17.42
Q_{50} (mm d^{-1})	0.95	1.24	0.90
Q_{95} (mm d^{-1})	0.35	0.34	0.22
CV_Q			
Spring	0.5	0.6	1.2
Summer	1.5	1.5	1.8
Autumn	1.4	1.2	1.7
Winter	0.6	0.5	0.9

Table 2: Summary of daily flow statistics for the three nested sites

Site	HW1	Bruntland Burn	Girnock
δ^2H precipitation			
Mean (‰)	NA	-54.6	NA
Min (‰)	NA	-145.9	NA
Med (‰)	NA	-49.8	NA
Max (‰)	NA	-12.3	NA
CV (%)	NA	47.5	NA
δ^2H stream water			
Mean (‰)	-56.8	-58.1	-59.1
Min (‰)	-70.3	-72.2	-81.8
Med (‰)	-56.9	-58.0	-59.0
Max (‰)	-48.0	-50.9	-50.6
CV (%)	6.6	5.3	6.2
lc- excess precipitation			
Mean (‰)	NA	-1.0	NA
SD (‰)	NA	5.2	NA
Min (‰)	NA	-15.4	NA
Med (‰)	NA	-1.1	NA
Max (‰)	NA	18.9	NA
lc- excess stream water			
Mean (‰)	0.9	1.6	1.8
SD (‰)	1.9	1.9	1.9
Min (‰)	-5.1	-6.4	-4.2
Med (‰)	1.2	1.8	1.9
Max (‰)	5.5	9.0	7.9
lc-excess summer			

Med (‰)	0.5	1.8	1.2
SD (‰)	1.6	1.3	1.9
lc-excess winter			
Med (‰)	2.6	2.8	3.6
SD (‰)	1.2	1.6	1.1
Data capture			
n	350	407	370
% capture	81%	94%	86%

Table 3: Summary statistics for stable isotopes for the three nested sites (SD is standard deviation, CV is the coefficient of variation). Data capture shows the number of samples collected (n) from each site and % captures shows this number as a percentage of the total number of sampling days (432 days).

	HW1	**Bruntland Burn**	**Girnock**
Derived DOC			
Max (mg l^{-1})	22.1	11.5	20.2
Min (mg l^{-1})	4.7	2.0	1.6
Mean (mg l^{-1})	9.4	4.9	6.0
Median (mg l^{-1})	8.9	4.5	5.3
CV	37.3	38.0	52.4
n	343	385	385
Measured DOC			
Max (mg l^{-1})	20.8	11.1	19.4
Min (mg l^{-1})	4.0	2.4	2.5
Mean (mg l^{-1})	9.7	5.3	6.6
Median (mg l^{-1})	9.6	5.0	6.0
CV	36.1	37.2	50.1
n	124	111	120

Table 4: Summary statistics for daily DOC concentrations for the three sites. Derived DOC refers to values either modelled using MLR (and kriging) or derived using FDOM-DOC relationship. Measured DOC refers to values that have been analysed in the laboratory.

Event number	Catchment	Discharge			DOC			Lag time (hours)	HI	Hysteresis direction
		Q_{pre} (mm 15min^{-1})	Q_{peak} (mm 15min^{-1})	Q increase (%)	DOC_{pre} (mg l^{-1})	DOC_{peak} (mg l^{-1})	DOC increase (%)			
1	HW1	0.008	0.036	321	5.82	7.20	24	16.5	-0.68	A
	BB	0.010	0.040	293	3.66	5.60	53	4.5	-0.59	A
2	HW1	0.011	0.091	735	7.08	7.64	8	0.25	-0.35	C
	BB	0.014	0.108	678	4.80	6.16	28	3	-0.40	A
3	HW1	0.015	0.030	100	5.30	6.23	18	6	-0.49	A
	BB	0.017	0.042	146	4.00	5.04	26	3.5	-0.40	A
4	HW1	0.005	0.029	490	9.00	11.39	27	16.75	-0.47	A
	BB	0.005	0.054	905	4.79	7.23	51	3.5	-0.28	A
5	HW1	0.008	0.037	361	10.03	11.22	12	4.5	-0.38	A
	BB	0.008	0.060	664	5.22	7.28	40	4	-0.23	A
6	HW1	0.004	0.021	397	7.99	10.06	26	3.25	-0.48	A
	BB	0.006	0.028	375	2.98	6.60	121	7.5	-0.52	A
7	HW1	0.005	0.018	251	8.23	10.80	31	13	-0.46	A
	BB	0.005	0.023	353	3.82	7.20	89	8.5	-0.75	A
8	HW1	0.003	0.020	662	12.18	18.95	56	5	-0.69	A
	BB	0.002	0.016	641	4.96	8.47	71	2.5	-0.64	A
9	HW1	0.003	0.039	1103	15.94	19.33	21	16.25	-0.32	A
	BB	0.003	0.025	855	4.66	10.42	123	33.5	-0.33	A
10	HW1	0.004	0.141	3424	15.84	19.87	25	3.75	-0.52	A
	BB	0.004	0.192	4483	7.12	11.99	68	4.75	-0.85	A
11	HW1	0.010	0.028	170	13.83	17.04	23	3.75	-0.73	A
	BB	0.011	0.036	246	7.52	9.75	30	1	-0.26	A
12	HW1	0.005	0.033	557	12.09	14.75	22	3.75	-0.67	A
	BB	0.005	0.019	317	4.23	7.58	79	7.25	-0.79	A
Mean	HW1	0.007	0.040	714	10.28	12.87	24	7.73	-0.52	
	BB	0.007	0.050	830	4.81	7.78	65	6.96	-0.50	

Table 5: Event hysteresis statistics for HW1 and BB. HI = hysteresis index, A = anticlockwise, C = clockwise.

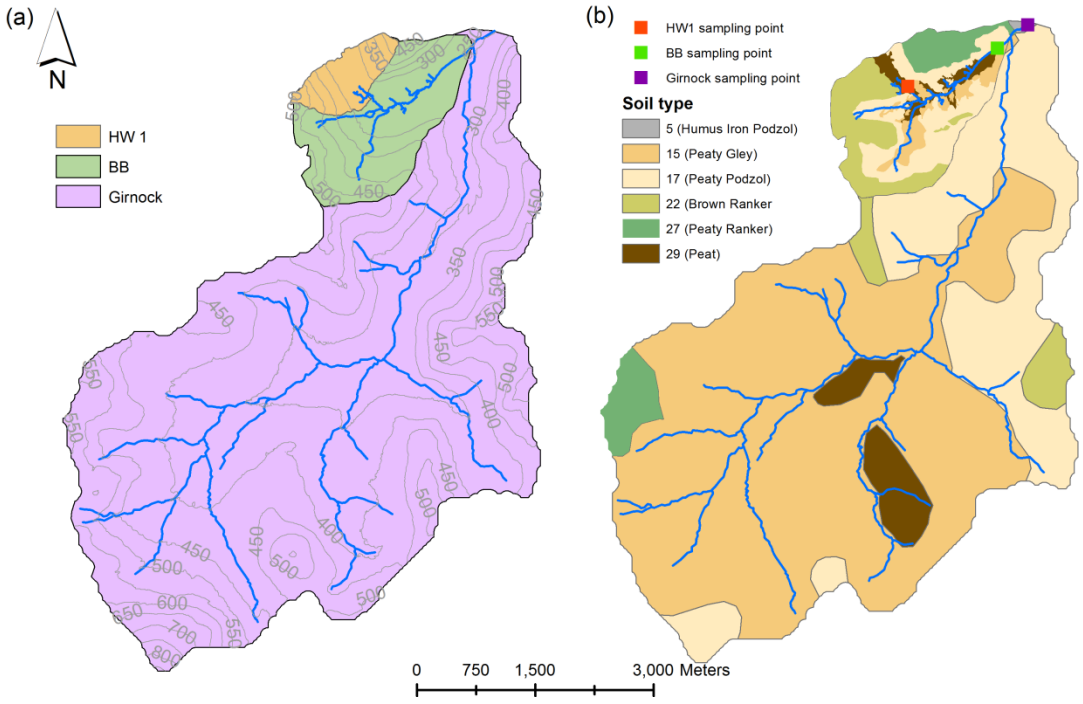

1012

1013 **Figure 1:** (a) Outlines of the three nested catchments and contour lines (b) Sampling sites and

1014 dominant soil types in each of the catchments.

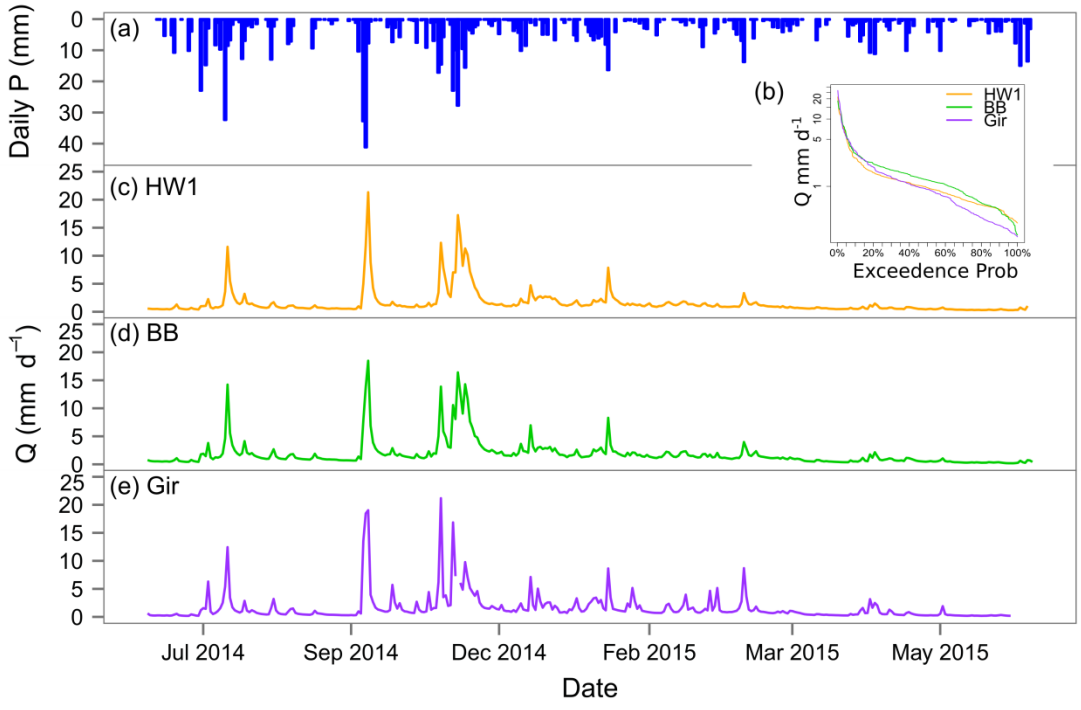

1015

1016 **Figure 2:** Daily time series of (a) precipitation (c) flow for HW1 (d) flow for the Bruntland

1017 Burn (e) flow for the Girnock. Flow duration curves for all 3 sites are shown in (b).

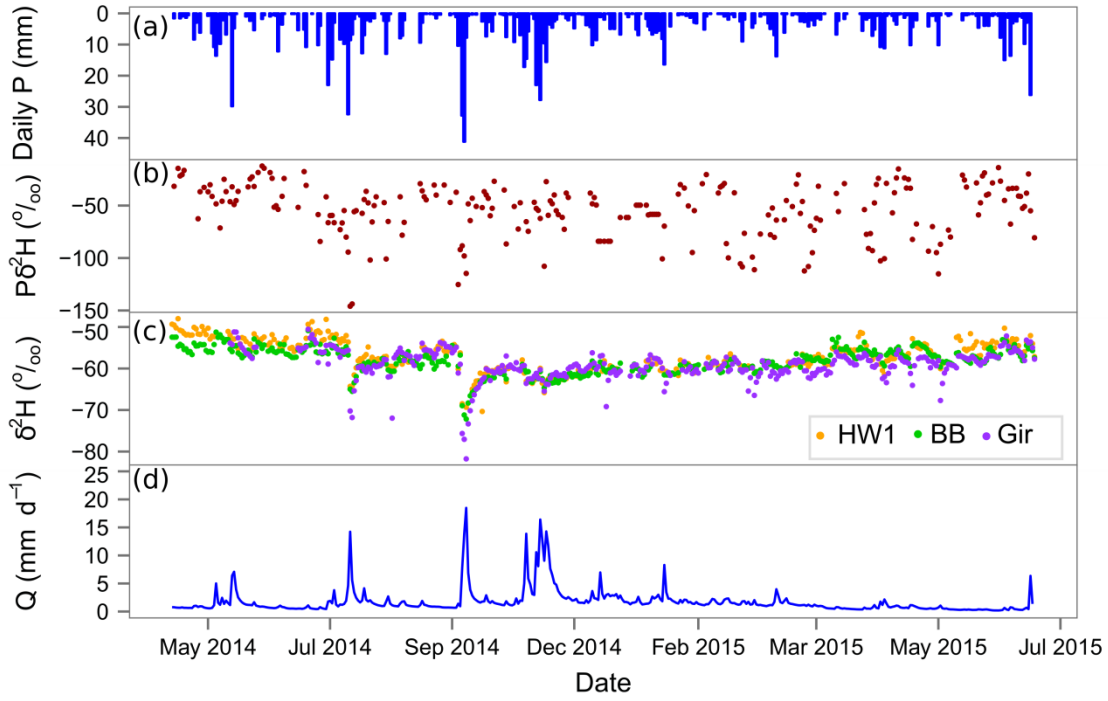

1018

1019 **Figure 3:** Daily time series of (a) precipitation (b) precipitation δ^2H signatures measured in

1020 the BB (c) stream water δ^2H signatures for the three sites (d) discharge of the Bruntland Burn.

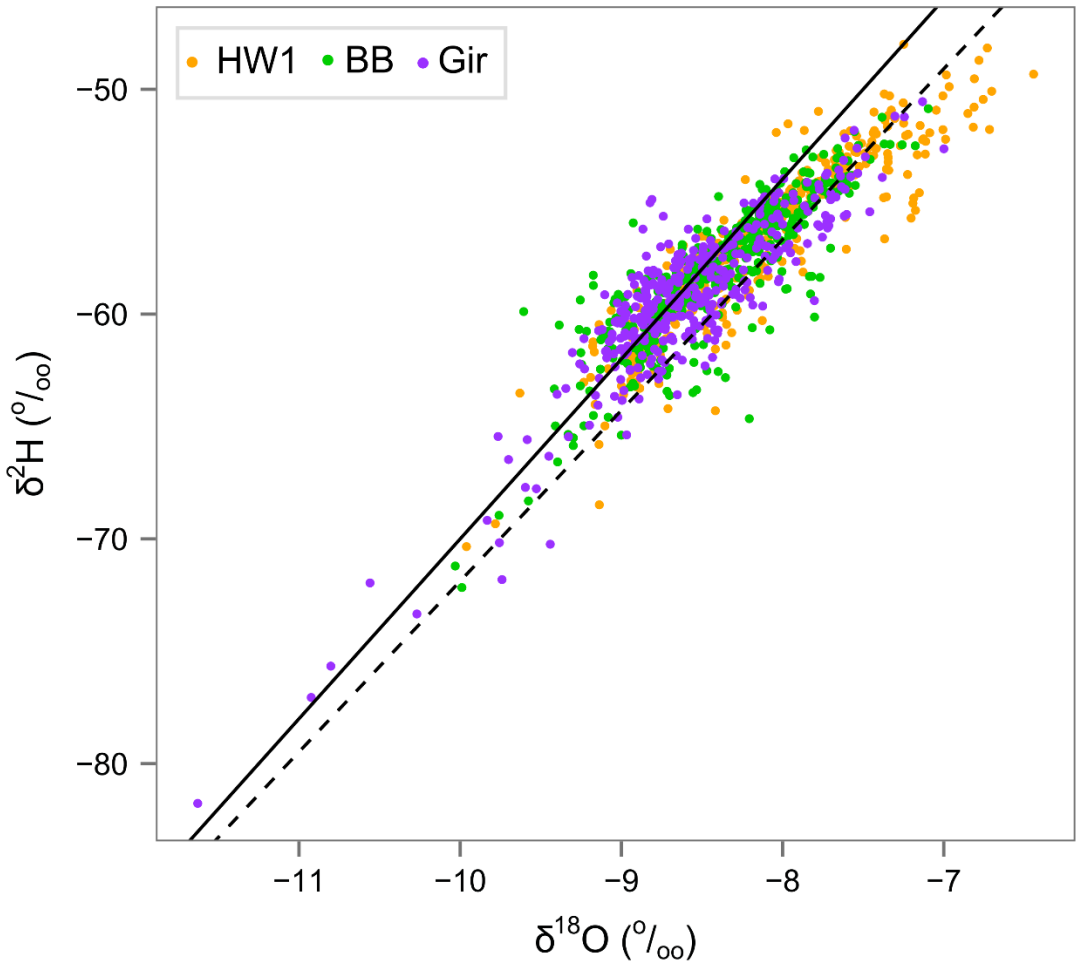

1021

1022 **Figure 4**: Stream water stable isotopes at the three sites plotted along the Global Meteoric

1023 Water Line (solid line) and Local Meteoric Water Line (dashed line)

1024

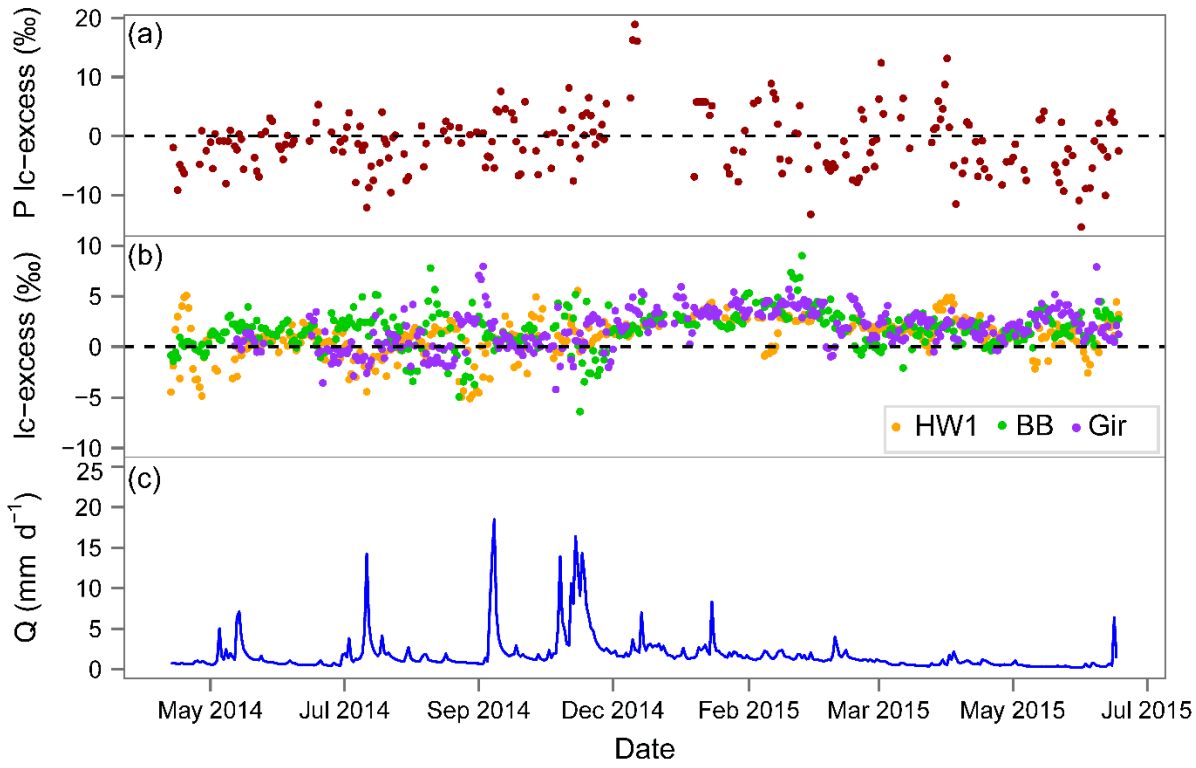

1025

1026 **Figure 5:** Timeseries of (a) precipitation lc-excess for the three sites (b) stream water lc-excess

1027 for the three sites (c) discharge at the Bruntland Burn.

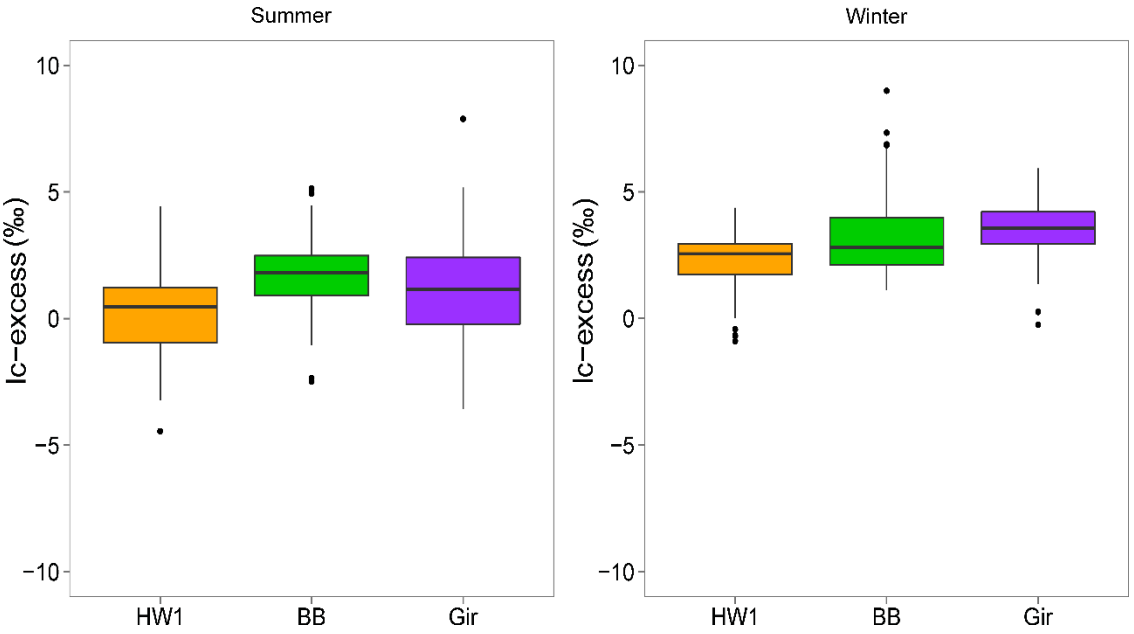

1028

1029

Figure 6: Boxplots of lc-excess values for the three sites in summer (June, July and August) and in winter (December, January, February).

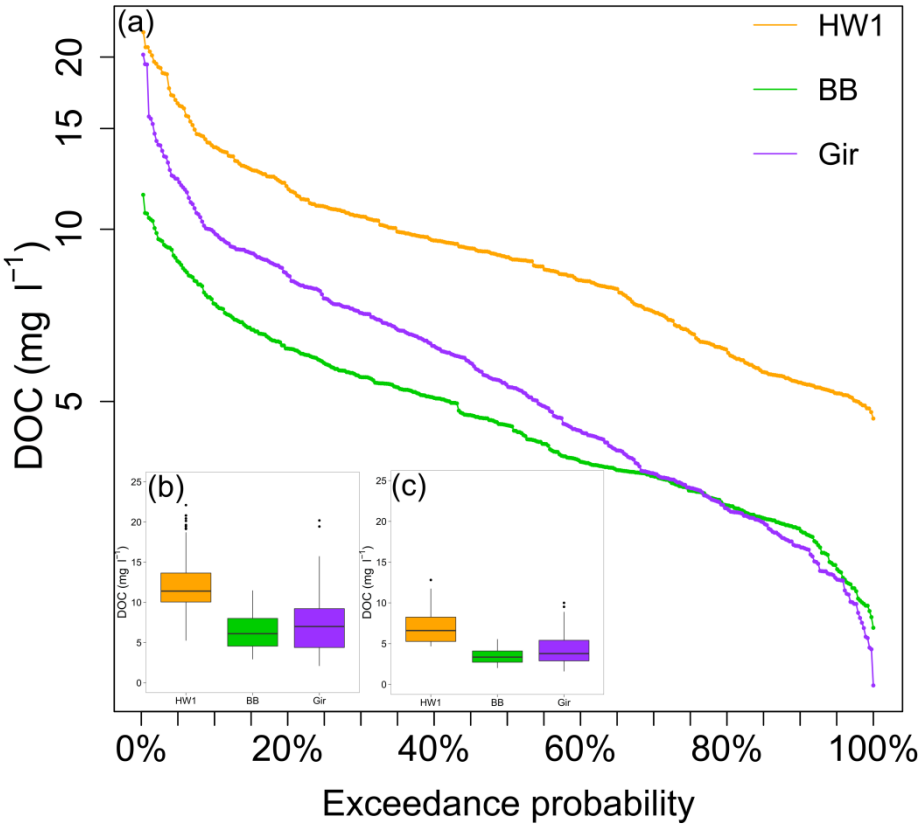

Figure 7: (a) Daily DOC concentration exceedance curves for the three sites (b) box plots of daily DOC concentration for the three sites in summer (June, July and August) (c) box plots of daily DOC concentration for the three sites in winter (December, January and February).

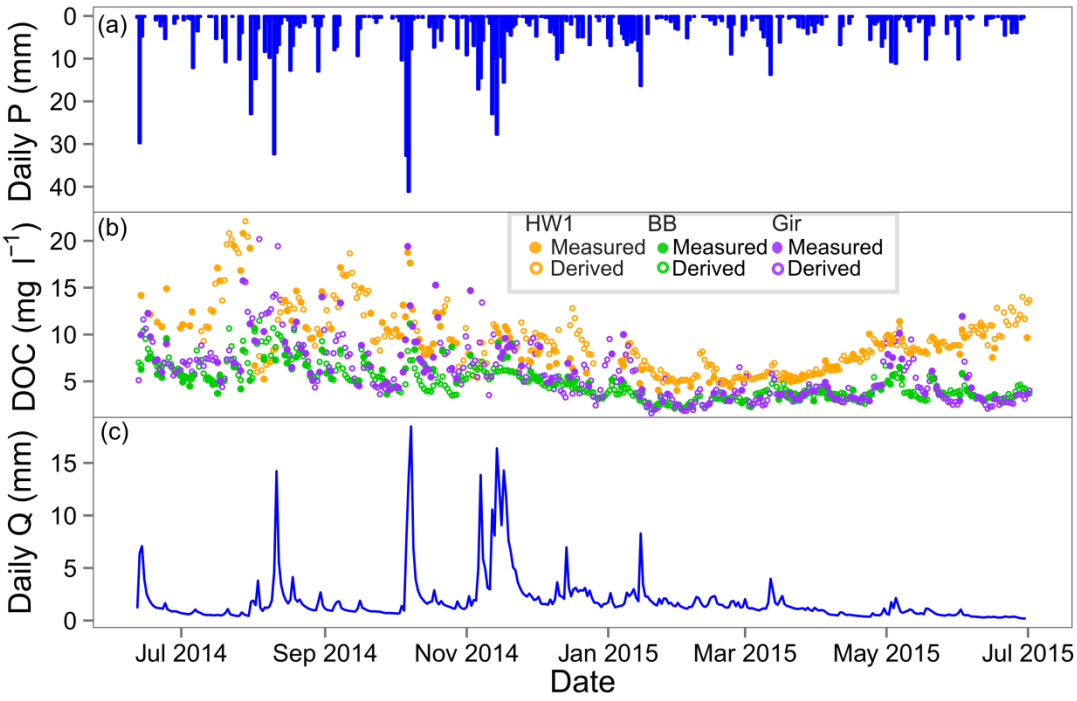

1037

1038 **Figure 8:** Timeseries of (a) daily precipitation (b) daily DOC for the three sites. The filled
1039 points are discrete water samples analysed in the laboratory for DOC and unfilled points
1040 represent either modelled DOC using MLR with discharge and temperature (and kriging) or
1041 DOC derived from FDOM. Up until 23/11/14, unfilled points for HW1 represent modelled
1042 DOC concentration and the remaining time series represents the DOC values derived from
1043 FDOM data. Unfilled points for the BB are mainly the DOC value derived from FDOM data
1044 apart from between 14/01/15 – 5/03/15 when DOC was modelled. Unfilled points for GIR are
1045 DOC concentrations modelled using MLR with discharge and temperature (and kriging). (b)
1046 daily discharge data as represented by the Bruntland Burn flow data.

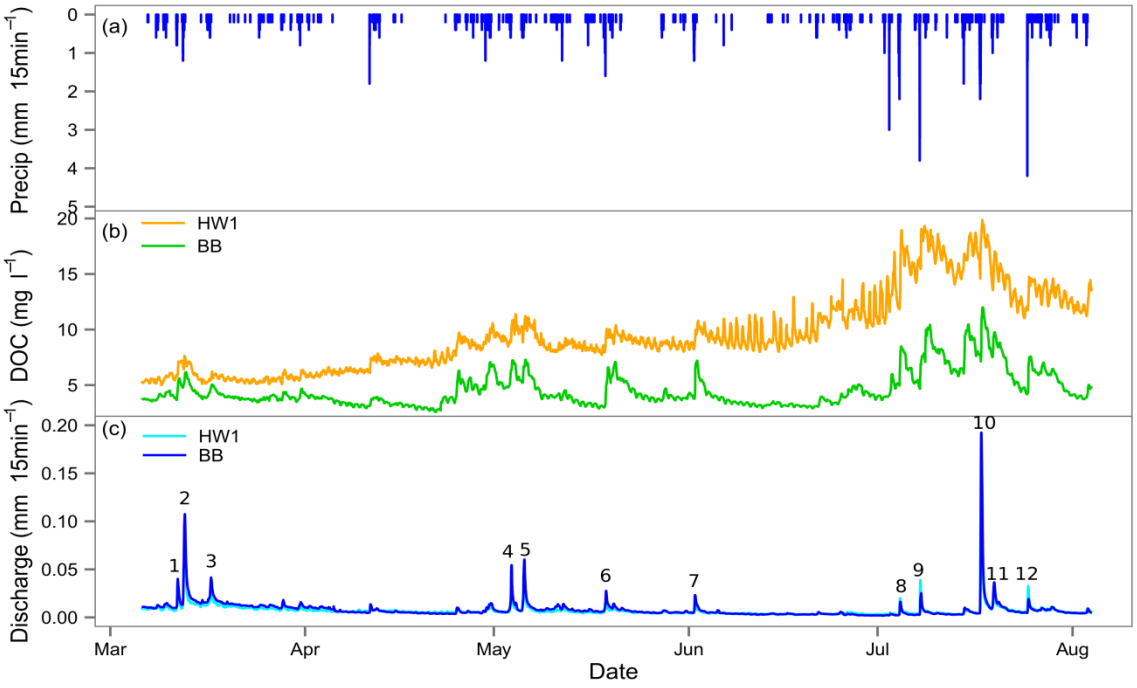

1047

1048 **Figure 9:** Time series of (a) 15 minute precipitation (b) high frequency DOC derived from
1049 FDOM measurements for HW1 and the BB (c) 15 minute discharge for HW1 and the BB. The
1050 numbers above the peaks show the specific events analysed (see Figure 10 and Table 5).

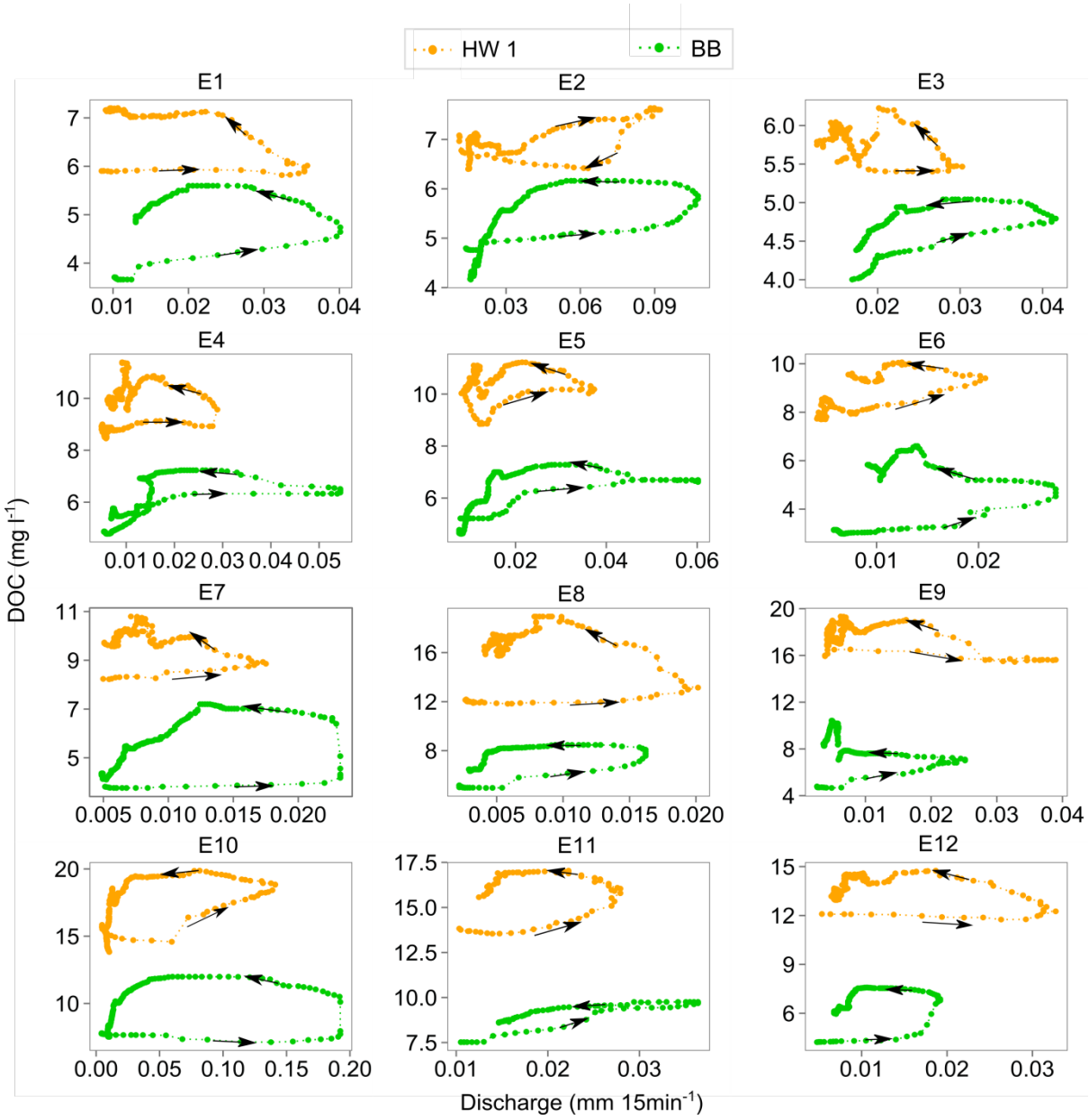

1051

1052 **Figure 10:** Hysteresis loops for the 12 events captured for HW1 (orange) and BB (green)

1053

1054

1055

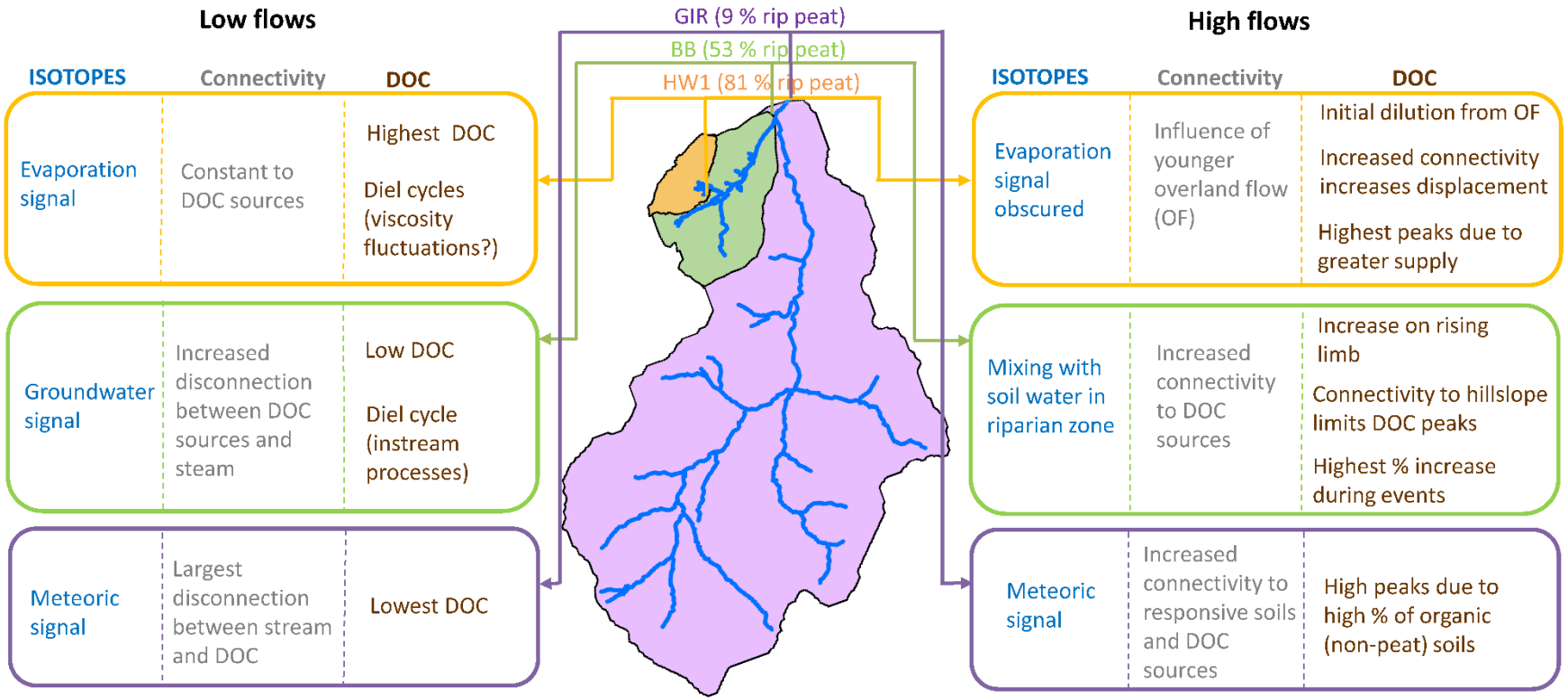

Figure 11: Conceptual diagram synthesising the relative importance of spatio-temporal isotope and DOC processes at the outlets of the three catchment scales.